HHS Public Access

Author manuscript

Nat Immunol. Author manuscript; available in PMC 2009 November 01.

Published in final edited form as:

Nat Immunol. 2009 May ; 10(5): 540–550. doi:10.1038/ni.1725.

HoxC4 binds to the *Aicda* promoter to induce AID expression, class switch DNA recombination and somatic hypermutation

Seok-Rae Park[1], **Hong Zan**[1], **Zsuzsanna Pal**, **Jinsong Zhang**, **Ahmed Al-Qahtani**, **Egest J Pone**, **Zhenming Xu**, **Thach Mai**, and **Paolo Casali**

Institute for Immunology, School of Medicine and School of Biological Sciences, University of California, 3028 Hewitt Hall, Irvine, CA 92697-4120, USA.

Abstract

AID is critical for immunoglobulin class switch DNA recombination (CSR) and somatic hypermutation (SHM). Here we showed that AID expression was induced by the HoxC4 homeodomain transcription factor, which bound to a highly conserved HoxC4-Oct site in the *Aicda* promoter. This site functioned in synergy with a conserved Sp-NF-κB-binding site. HoxC4 was preferentially expressed in germinal center B cells and was upregulated by CD154:CD40 engagement, lipopolysaccharide and interleukin-4. HoxC4 deficiency resulted in impaired CSR and SHM, due to decreased AID expression and not other putative HoxC4-dependent activity. Enforced expression of AID in *Hoxc4*$^{-/-}$ B cells fully restored CSR. Thus, HoxC4 directly activates the *Aicda* promoter, thereby inducing AID expression, CSR and SHM.

CSR and SHM are critical for the maturation of antibody responses to foreign and self-antigens. CSR recombines switch (S) region DNA located upstream of constant heavy chain (C_H) region exons, thereby changing immunoglobulin (Ig) C_H regions and endowing antibodies with new biological effector functions. SHM introduces mainly point mutations in Ig variable regions, thereby providing the structural substrate for selection of higher affinity antibody mutants by antigen. In spite of the recent advances made in the identification of some factors involved in CSR and SHM, the intimate mechanisms of these processes remain elusive. Both CSR and SHM require activation-induced cytidine deaminase (AID), which is expressed by activated B cells, mainly in germinal centers (GCs) of peripheral lymphoid organs1,2. AID initiates CSR and SHM by deaminating dC residues to yield dU:dG mispairs in DNA3–8. These dU:dG mispairs trigger DNA repair processes entailing introduction of mutations in V(D)J regions or DNA breaks, including double-stranded DNA breaks, which lead to non-classic non-homologous end-joining and CSR3,5,9–14.

Correspondence should be addressed to P.C. (pcasali@uci.edu).

[1]These authors contributed equally to this work.

AUTHOR CONTRIBUTIONS

H.Z. and S.-R.P. contributed equally to this work; S.-R.P., H.Z., Z.P., J.Z., T.M., E.J.P. and A.A.-Q. performed the experiments; Z.X. helped designing experiments, discussed the results and read and provided comments on the manuscript; H.Z. designed the experiments, analyzed the data and prepared the manuscript; P.C. designed the experiments, analyzed the data, supervised the work and prepared the manuscript.

The mechanisms governing the transcriptional regulation of the gene encoding AID (*AICDA* in the human and *Aicda* in the mouse) remain to be elucidated. A conserved region in the first intron of *Aicda* containing two E-boxes, the consensus sequence for E2A (http://www.signaling-gateway.org/molecule/query?afcsid=A000804) binding, has been suggested to contribute to *Aicda* transcription regulation through recruitment of the E2A helix-loop-helix (HLH) transcription factor E47 and the inhibitor of DNA-binding HLH protein Id3, respectively15. Pax5 has been suggested to cooperate with E2A proteins in controlling *Aicda* transcription16. However, this could not be confirmed by another study, which rather suggested a role for the Sp1 family of ubiquitous zinc-finger transcription factors. These regulate various promoters by binding to dGdC, dGdA or dGdT boxes, in activating the *Aicda* promoter17.

Hox proteins are highly conserved HLH homeodomain-containing transcription factors that regulate cellular differentiation and organogenesis18,19. *Hox* genes, which are chromosomally clustered, are expressed in a temporally and spatially regulated fashion20,21. Among human *HOX*, *HOXC* genes, particularly *HOXC4*, are predominantly expressed in lymphoid cells22. *HOXC4* gene expression increases through sequential stages of B cell development22–25, from non-committed hematopoietic progenitors in the bone marrow to mature B cells in the periphery, particularly when activated and proliferating. Malignant B cells including mantle cell lymphoma, Burkitt's lymphoma and B cell chronic lymphocytic leukemia, express aberrant AID26, 27 and abundant HoxC422,28. HoxC4 induces the human 3' E_{α} enhancer elements, particularly DNAse I hypersensitive sites hs1,2, in a B cell development stage-specific fashion25. HoxC4 binds to a HoxC4-Oct motif 5'-ATTTGCAT-3' site in hs1,224,25, which is conserved in the human, mouse, rat and rabbit, and synergizes with the Oct1/Oct2 (http://www.signaling-gateway.org/molecule/query?afcsid=A001704) homeodomain proteins and the OcaB (http://www.signaling-gateway.org/molecule/query?afcsid=A001696) co-activator to induce this enhancer in B cells24,25. *HOXC4* expression is induced by stimuli that induce GC B cell differentiation and *AICDA* expression24,25, such as CD154 (http://www.signaling-gateway.org/molecule/query?afcsid=A000536) and interleukin 4 (IL-4) (http://www.signaling-gateway.org/molecule/query?afcsid=A001262), suggesting a role of HoxC4 in CSR and SHM.

In this study, we tested the hypothesis that HoxC4 regulates AID expression in human and mouse B cells. We showed that HoxC4 bound to a HoxC4-octamer motif in the *AICDA* and *Aicda* promoters that is conserved in humans, chimps, mice, rats, dogs and cows. Binding of HoxC4 to this *cis*-element activated the AID gene promoter and induced AID expression, thereby inducing CSR and SHM. In this function, HoxC4 synergized with an equally conserved upstream Sp-NF-κB site in the AID gene promoter.

RESULTS

HoxC4 and AID are induced in GC B cells

We have shown that HoxC4 is upregulated in human $IgD^{-}CD38^{+}$ GC B cells24,25, which express AID and undergo CSR and SHM. Stimulation of human $IgD^{+}CD38^{-}$ naive B cells with an agonistic CD40 monoclonal antibody (mAb) and huIL-4 upregulated HoxC4 and induced AID expression24,25. We further analyzed the expression of *Hoxc4* and *Aicda* in

bone marrow, thymus, spleen, Peyer's patches, liver and heart of wild-type C57BL/6 mice. Real-time quantitative qRT-PCR revealed that like *Aicda*, *Hoxc4* was preferentially expressed in the spleen and Peyer's patches, which contain a large proportion of hypermutating and switching B cells, but not in non-lymphoid organs, such as the liver or the heart (Fig. 1a). To further address the correlation between HoxC4 and AID expression, we isolated $PNA^{hi}B220^{+}$ GC and $PNA^{lo}B220^{+}$ (non-GC) B cells from spleen of 8- to10-week-old C57BL/6 mice, 14 d after immunized with 4-hydroxy-3-nitrophenyl acetyl coupled to chicken γ-globulin (NP_{16}-CGG), and analyzed the amount of the two proteins, as well as PCNA, which is a multi-functional protein critical for DNA replication and repair and is highly expressed in actively dividing cells. HoxC4 was specifically expressed in $PNA^{hi}B220^{+}$ GC B cells, where AID and PCNA were also highly expressed (Fig. 1b). Stimulation of mouse spleen B cells with bacterial lipopolysaccharide (LPS) and IL-4 or CD154 and IL-4, which induce GC B cell differentiation and *Aicda* expression upregulated *Hoxc4* expression by 10 to 15 fold (Fig. 1c) and induced CSR to IgG1 (not shown), indicating that HoxC4 plays a role in inducing AID expression.

HoxC4 deficiency impairs antibody response to NP-CGG

We used $Hoxc4^{-/-}$ mice to address the role of HoxC4 in CSR and SHM. Two lines of HoxC4-deficient mice were independently generated and homozygous mutants of both lines displayed esophageal defects and abnormal cervical and thoracic vertebral development and suffered high post-natal mortality rates29,30. In these mice, the expression of *Hoxc5* and *Hoxc6*, which lie in the same gene cluster as *Hoxc4*, was reduced, likely due to the neighboring impact of the neomycin-selection (neo^{r}) cassette inserted into the *Hoxc4* locus29,30. To obviate this, a third $Hoxc4^{-/-}$ strain, in which the neo^{r} cassette was deleted by Cre recombinase through two flanking *lox*P sites in the germline (Supplementary Fig. 1 online), thereby leaving *Hoxc5* and *Hoxc6* expression unaltered (Boulet and Capecchi unpublished). Such mice were since lost, but frozen $Hoxc4^{+/-}$ sperm on the C57BL/6 background was preserved. Using $Hoxc4^{+/-}$ sperm, we re-derived $Hoxc4^{+/-}$ mice by *in vitro* fertilization and bred them to obtain $Hoxc4^{-/-}$ mice. These $Hoxc4^{-/-}$ mice are born at Mendelian ratio, do not suffer the high post-natal mortality rate of the earlier HoxC4-deficient mouse lines29,30 and develop to adulthood.

In non-immunized $Hoxc4^{-/-}$ mice, serum IgM titers were normal. However, the average serum IgG1 concentration was less than 0.6 mg/ml, as compared to 1.2 mg/ml in their $Hoxc4^{+/+}$ littermates (not shown), suggesting an impairment of CSR. We immunized four pairs of 8–10-week-old littermate $Hoxc4^{-/-}$ and $Hoxc4^{+/+}$ mice with NP_{16}-CGG and analyzed blood from these mice for IgM and IgG1 titers, NP_{30}-binding IgM and IgG1, and high-affinity NP_{3}-binding IgM and IgG1 (Fig. 2a). Total IgM and NP_{30}-binding IgM were not significantly different in $Hoxc4^{-/-}$ from $Hoxc4^{+/+}$ mice. $Hoxc4^{-/-}$ mice, however, showed some decrease in NP_{3}-binding IgM and significantly lower total IgG1, NP_{30}-binding IgG1 as well as high affinity NP_{3}-binding IgG1 titers. The defective antibody response to NP-CGG did not reflect an altered plasma cell or memory B cell development, as the proportions of $B220^{lo}CD138^{+}$ cells and $CD38^{hi}$ B cells among NP-binding IgG1 B cells in NP_{16}-CGG-immunized $Hoxc4^{-/-}$ mice were comparable to those of their $Hoxc4^{+/+}$

littermates (Fig. 2b). Rather, it reflected the decreased overall IgG1 levels and, together with the slightly lower NP_3-binding IgM activity, a decreased binding affinity for NP_3.

HoxC4 deficiency does not alter GC formation

The defective antibody response to NP-CGG in *Hoxc4*$^{-/-}$ mice was not due to obvious defects in lymphoid differentiation. In these mice, the size of the spleen, and the number and the size of Peyer's patches were comparable to those in *Hoxc4*$^{+/+}$ mice (not shown). Moreover, the number of B and T cells, the proportion of $CD4^+$ T cells, and death of B and T cells in the spleen and Peyer's patches, as analyzed by staining with 7-amino-actinomycin (7-AAD), were also comparable to those of *Hoxc4*$^{+/+}$ mice (Fig. 3a–d). After stimulation with LPS and IL-4, *Hoxc4*$^{-/-}$ B lymphocytes were comparable in cell cycle, as analyzed by propidium iodide (PI) staining, and cell division rate, as measured by carboxyfluorescein diacetate succinimidyl ester (CFSE) vital dye incorporation, to *Hoxc4*$^{+/+}$ cells (Fig. 3e,f). In *Hoxc4*$^{-/-}$ mice, the number and architecture of the GCs in the spleen, the proportions of proliferating B cells, as shown by *in vivo* bromodeoxyuridine (BrdU) incorporation, and the proportion of PNA^{hi} GC B cells in both spleen and Peyer's patches were comparable to those of *Hoxc4*$^{+/+}$ mice (Fig. 3g,h,i), suggesting that the defective antibody response to NP_{16}-CGG in *Hoxc4*$^{-/-}$ mice reflected an intrinsic impairment of the CSR and SHM machineries.

HoxC4 deficiency impairs CSR and SHM

To determine the impact of HoxC4 deficiency on CSR, we stimulated spleen B cells with LPS (to induce switching to IgG2b and IgG3) or LPS or CD154 with IL-4 (to IgG1 and IgE), LPS or CD154 with IFN-γ (http://www.signaling-gateway.org/molecule/query?afcsid=A001238) (to IgG2a) and LPS or CD154 in the presence of transforming growth factor-β1 (TGF-β1, http://www.signaling-gateway.org/molecule/query?afcsid=A002271), IL-5, IL-4 and anti-δ-mAb-dextran (to IgA). After 4 d, in cultures stimulated with LPS or LPS and cytokines, surface $IgG1^+$, $IgG2a^+$, $IgG2b^+$, $IgG3^+$, IgA^+ and IgE^+ *Hoxc4*$^{-/-}$ B cells were decreased by 54%, 49%, 46%, 36%, 43% and 57%, respectively, as compared to *Hoxc4*$^{+/+}$ B cell cultures (Supplementary Fig. 4a online); in cultures stimulated with CD154 and cytokines, surface $IgG1^+$, $IgG2a^+$ and IgE^+ *Hoxc4*$^{-/-}$ B cells were decreased by 49%, 69% and 79%, respectively. Accordingly, aftre 7 d, IgG1, IgG2a, IgG2b, IgG3, IgA and IgE secreted by *Hoxc4*$^{-/-}$ B cells stimulated with LPS or LPS and cytokines were decreased by as much as 48%, 55%, 37%, 35%, 40% and 66%, respectively (Fig. 4a). Impaired CSR in *Hoxc4*$^{-/-}$ B cells was not due to altered proliferation, as after 2, 3 or 4 d of culture with LPS and IL-4 or CD154 and IL-4, *Hoxc4*$^{-/-}$ B cells completed the same number of divisions, as their *Hoxc4*$^{+/+}$ counterparts (Fig. 3f, Fig.4b), or altered plasma cell differentiation, as after 4 d of culture with LPS, LPS and IL-4 or CD154 and IL-4, the number of $CD138^+B220^{lo}$ plasma cells emerging from *Hoxc4*$^{-/-}$ B cells was comparable to that of their *Hoxc4*$^{+/+}$ counterparts (Fig. 4c). Accordingly, the expression of transcription factors Blimp-1 and IRF-4, which are critical in plasma cell differentiation, were comparable in *Hoxc4*$^{-/-}$ and *Hoxc4*$^{+/+}$ B cells, as determined by real-time qRT-PCR, 5 d after stimulation with LPS and IL-4 (data not shown). Further, reduced CSR in *Hoxc4*$^{-/-}$ B cells was not due to an impairment of germline I_H-C_H transcription, which is necessary for CSR. Real-time qRT-PCR showed that germline I_μ-C_μ, $I_\gamma3$-$C_\gamma3$, $I_\gamma1$-$C_\gamma1$, $I_\gamma2b$ -$C_\gamma2b$, $I_\gamma2a$-$C_\gamma2a$, I_ε-C_ε and I_α-C_α

transcripts in *Hoxc4*$^{-/-}$ B cells stimulated with LPS or LPS and cytokines for 3 d were comparable to those of their *Hoxc4*$^{+/+}$ B cell counterparts (Fig. 5, Supplementary Fig. 3), while the post-recombination I_μ-C_H transcripts, which are generated by CSR, were significantly decreased in *Hoxc4*$^{-/-}$ B cells, by as much as 89.2%. Thus, HoxC4-deficiency impairs CSR to all isotypes without affecting germline I_H-C_H transcription.

To determine the impact of HoxC4 deficiency on SHM, we analyzed the J_H4-iE_μ sequence downstream of rearranged $V_{J558}DJ_H4$ DNA in PNA^{hi} B220$^+$ GC B cells from Peyer's patches of 3 pairs of 12-week-old non-immunized littermate *Hoxc4*$^{-/-}$ and *Hoxc4*$_{+/+}$ mice. In these mice, the proportions of Peyer's patch PNA^{hi} B220$^+$ GC B cells were comparable (Fig. 3h). Analysis of 324 and 319 J_H4-iE_μ intronic DNA sequences (720 bp) from *Hoxc4*$^{-/-}$ and *Hoxc4*$^{+/+}$ mice showed a decrease in mutations in *Hoxc4*$^{-/-}$ mice by 59% ($P < 0.00001$) (Fig. 6a). The decreased mutation frequency was associated with a comparable reduction in mutations at dG:dC and dA:dT (Supplementary Fig. 4, online) and was not due to impaired transcription of the rearranged $V_{J558}DJ_H$ genes, as shown by specific real-time qRT-PCR in Peyer's patches B cells of these *Hoxc4*$^{-/-}$ mice, as compared to their *Hoxc4*$^{+/+}$ littermates (Fig. 6b). Thus, HoxC4 deficiency significantly impairs SHM, without altering the spectrum of the residual mutations or V_HDJ_H transcription.

HoxC4 deficiency impairs AID expression

CSR and SHM require transcription of the *Igh* locus and AID expression. The significant reduction of CSR and SHM, together with the normal amounts of mature V_HDJ_H-C_μ and germline I_H-C_H transcripts in *Hoxc4*$^{-/-}$ B cells prompted us to hypothesize a modulation of AID expression by HoxC4. We stimulated spleen *Hoxc4*$^{+/+}$ and *Hoxc4*$^{-/-}$ B cells with LPS and IL-4, or CD154 and IL-4 for 0, 12, 24, 48 and 72 h. *Aicda* mRNA expression could be detected by real-time qRT-PCR as early as 24 h and peaked within 48–72 h of stimulation in *Hoxc4*$^{+/+}$ B cells. In *Hoxc4*$^{-/-}$ B cells, *Aicda* expression was reduced by more than 70%, after 72 h of stimulation (Fig. 7a). Decreased *Aicda* transcripts were associated with a significant decrease in AID protein (Fig. 7b), further suggesting that HoxC4 regulates *Aicda* expression.

Transcription factor binding to the *Aicda* promoter

To address the possibility that HoxC4 modulates *Aicda* expression by binding to a *cis*-regulatory element of this gene, we analyzed the sequence upstream of the putative transcriptional initiation site of the *Aicda* gene (Supplementary Fig. 5 online). In this, we identified eight motifs conserved in humans, chimps, mice, rats, dogs and cows (Supplementary Fig. 5 online, C1–C8). The first six motifs did not fulfill the minimal criteria for known transcription factor-binding sites by weight matrix search using Match™ (threshold score, 0.75). The last two (C7 and C8) consisted of a HoxC4 or Oct-binding 5'-ATTTGAAT-3' site (residues −29 to −22 in the human and mouse) (scores: 1.0 for HoxC4 and 0.93 for Oct), virtually identical to the conserved HoxC4-Oct motif we showed to be critical in inducing the human *IGH* 3' E_α enhancer elements24,25, and an upstream Sp-NF-κB 5'-GGGGAGGAGCC-3' site (residues −57 to −47 in the human and mouse)17 (scores: 0.93 for Sp1/Sp3 and 0.96 for NF-κB). This was first suggested to be a Pax5-binding site16, but it did not satisfy, in our analysis, the minimal requirement for such a binding site (score:

0.61). Both the putative HoxC4-Oct- and the Sp-NF-κB-binding sites are identical in all six species analyzed.

To determine the role of the –349 to –1 *Aicda* promoter region (*AID-Pro*) in the regulation of *Aicda* transcription, we constructed luciferase gene reporter pGL3 vectors consisting of the 349 bp *AID-Pro* and/or the 490 bp flanking 5'-region (5'R) (Fig. 7c) upstream of the luciferase gene, combined with nil, conserved region1 (*cr1*) and/or *cr2*, which lie in the first intron in the *Aicda*15,16. We used these vectors to transfect human Ramos B cells, which spontaneously express *AICDA* and undergo SHM, and mouse CH12F3-2A B cells, which express *Aicda* and undergo CSR upon stimulation by LPS, IL-4 and TGF-β1. We cultured these B cells and measured luciferase activity after 16 h (Ramos) or 24 h (CH12F3-2A). The pGL3-5'R-AID-Pro construct, containing both the *Aicda* promoter and its flanking 5'-region, displayed an 11–15-fold higher activity than the empty pGL3-nil vector, in Ramos and CH12F3-2A B cells (Fig. 7d). In both Ramos and CH12F3-2A B cells, neither *cr1* nor *cr2* displayed substantial enhancer activity. In addition, while the pGL3-AID-Pro construct, containing only *Aicda* promoter, promoted transcription as efficiently as the pGL3-5'R-AID-Pro construct, the pGL3-5'R construct, which included only the flanking 5' region, displayed only an (background) activity comparable to that of the empty pGL3 vector in both Ramos and stimulated CH12F3-2A B cells. These experiments show that the 349 bp *AID-Pro* region displays full promoter activity, while neither *cr1* nor *cr2* enhances *Aicda* promoter activity in human or mouse B cells.

To address the specificity of the two evolutionarily conserved 5'-ATTTGAAT-3' and 5'-GGGGAGGAGCC-3' motifs, we performed gel electrophoretic mobility shift assays (EMSAs), using WT and mutated oligonucleotide probes encompassing residues −65 to −14 of the human *AICDA* promoter sequence and containing both the HoxC4-Oct and the Sp-NF-κB sites (Sp-Hox), or an oligonucleotide probe encompassing residues −65 to −44 of the *AICDA* promoter sequence containing the Sp-NF-κB site (Sp) (Supplementary Fig. 6a online). Incubation of nuclear extracts from human 4B6 B cells, which spontaneously express *AICDA* and undergo CSR, or Ramos B cells with the Sp-Hox probe gave rise to four major protein–DNA complexes, A, A’ and B, B’ (Supplementary Fig. 6b,c). These were specific for the binding of HoxC4-Oct and Sp-NF-κB, respectively. The mutated oligonucleotides Sp-Hox^{mut}, Sp^{mut}-Hox, or Sp^{mut}-Hox^{mut}, in which the HoxC4-Oct site, the Sp-NF-κB site, or both of the two sites were disrupted, respectively, failed to compete efficiently the formation of complexes B and B’, A and A’, or all the four complexes. These results were confirmed by EMSAs involving the mutated oligonucleotides as radiolabeled probes; Sp-Hox^{mut} gave rise only complexes B and B’, Sp^{mut}-Hox yielded only A and A’, and Sp^{mut}-Hox^{mut} gave rise to none of the four complexes. Incubation of 4B6 or Ramos B cell nuclear extracts with the Sp probe gave rise to three major protein-DNA complexes, C, C’ and C”, specific for binding of Sp-NF-κB. The binding specificity of HoxC4, Oct1 and Oct2 to the 5'-ATTTGAAT-3' site, and the binding specificity of Sp1, Sp3 and NF-κB to the 5'-GGGGAGGAGCC-3' site were further proved by supershift or inhibition of formation of the respective protein-DNA complexes by specific mAb to HoxC4 and specific Abs to Oct1, Oct2, Sp1, Sp3 or the p52 subunit of NF-κB. No supershift or inhibition of protein-DNA complex involving the Sp-Hox or the Sp probe could be achieved using the Pax5-specific

antibody. These experiments show that HoxC4, Oct1 and Oct2 bind specifically to the conserved 5'-ATTTGAAT-3' site, while Sp1, Sp3 and NF-κB, but not Pax5, bind specifically to the conserved 5'-GGGGAGGAGCC-3' site in the *AICDA* promoter.

Cis sites critical for *Aicda* promoter activation

To determine the contribution of the conserved HoxC4-Oct- and Sp-NF-κB-binding sites to the *Aicda* promoter activity, we constructed luciferase gene reporter vectors containing the mouse *Aicda* promoter sequence (residues −349 to −1), which was variously mutated or deleted at the HoxC4-Oct and/or the Sp-NF-κB site. In addition to the conserved HoxC4-Oct-binding 5'-ATTTGAAT-3' site, we identified a putative HoxC4-binding 5'-ATTT-3' site in the mouse and rat AID gene promoter (residues −155 to −158 of mouse *Aicda*), but not in the human, chimp or dog AID gene promoter (Supplementary Fig. 5 online). Deletion of this site (mut0) did not alter the *Aicda* promoter activity (Fig. 8a). By contrast, deletion of the Hoxc4-Oct motif (mut1) reduced promoter activity by 71%, 64% and 88% in LPS, IL-4 and TGF-b induced mouse CH12F3-2A B cells, human 4B6 and Ramos B cells, respectively. To determine the relative contribution of HoxC4- and Oct-binding to the promoter activity of the HoxC4-Oct motif as a whole, we mutated 5'-ATTTGAAT-3' to 5'-cTTTGAAT-3' (mut2), thereby disrupting the binding of HoxC4 but retaining Octbinding25, or to 5'-ATTTGccg-3' (mut3), thereby abrogating the binding of Oct1–Oct2 but not HoxC425. Mutation of the HoxC4 motif in the HoxC4-Oct site reduced transcription by 47%, 36%, or 55% in CH12F3-2A, 4B6 and Ramos B cells, respectively, while mutation of the Oct site reduced the promoter transcription by 28%, 21% and 55%, respectively. Thus, both the HoxC4 and the Oct motifs of the HoxC4-Oct site contribute to the *Aicda* promoter activity, as further confirmed by the up to 88% loss of *Aicda* promoter activity when the whole Hoxc4-Oct site was deleted (mut1). Further, mutation of the conserved Sp-NF-κB site to 5'-aaaaAGGAaa-3' (mut4) reduced promoter activity by 73%, 80% and 63% in CH12F3-2A, 4B6 and Ramos B cells, respectively. Accordingly, deletion of this site (mut5) resulted in 85%, 68% and 82% reduction in promoter activity in CH12F3-2A, 4B6 or Ramos B cells, respectively. Finally, deletion of the HoxC4-Oct site combined with mutation (mut6) or deletion (mut7) of the Sp-NF-κB site abrogated the *Aicda* promoter activity. These experiments show that the conserved HoxC4-Oct-binding site plays a major role in *Aicda* promoter activity and, together with the conserved Sp-NF-κB-binding site, is indispensable for full *Aicda* transcriptional activation.

To confirm the relevance of our EMSA and luciferase gene reporter experiments, we precipitated chromatin in human 4B6 and Ramos B cells using Abs to HoxC4, Oct1, Oct2, OcaB, Sp1, Sp3 or NF-κB (p52). In the DNA precipitated by all these Abs, we readily specified the *AICDA* promoter sequence (Fig. 8b,c). The specificity of these findings was further proved by our ability to readily detect *AICDA* or *Aicda* promoter DNA in ChIP assays involving human 2E2 B cells, which can be induced to express AID and undergo CSR by anti-CD40 mAb and cytokines, such as IL-4, mouse CH12F3-2A B cells, which can be induced to express AID and undergo CSR by LPS, IL-4 and TGF-β1, as well as spleen B cells from wild-type C57BL/6 mice activated by LPS and IL-4 or CD154 and IL-4. Induction of CSR in 2E2, CH12F3-2A B cells or primary mouse spleen B cells by these stimuli resulted in substantial *Hoxc4* expression and recruitment of HoxC4, Oct1, Oct2,

OcaB, Sp1, Sp3 and NF-κB to the *AICDA* and *Aicda* promoters. Because it has been suggested that Pax5 is (indirectly) recruited to the *Aicda* promoter16, we precipitated chromatin in these human and mouse B cells with an antibody to Pax5. In these immunoprecipitated DNA complexes, we readily detected the *AICDA* or *Aicda* promoter sequences, respectively. These findings show that HoxC4, Oct1, Oct2, OcaB, Sp1, Sp3 and NF-κB proteins are recruited to the *AICDA* and *Aicda* promoters in human and mouse B cells, respectively, which express AID and undergo CSR or SHM.

Enforced AID expression rescues CSR in *Hoxc4*$^{-/-}$ B cells

We then set up to demonstrate that the defective CSR in HoxC4-deficient B cells was actually due to impairment of AID expression and not other HoxC4-dependent activity. To this end, we enforced expression of AID in *Hoxc4*$^{-/-}$ B cells to restore CSR. We transduced LPS-activated spleen *Hoxc4*$^{+/+}$ and *Hoxc4*$^{-/-}$ B cells with TAC-*Aicda* or TAC control retroviral vector, stimulated them with LPS and IL-4 for 72 h and 96 h before analyzing CSR. The TAC control retroviral construct encoding human IL-2 receptor (hIL2RA, TAC antigen) and the AID-expression TAC-*Aicda* retroviral construct encoding AID and hIL-2RA were described15 (Supplementary Fig. 7, online). Consistent with what we saw in untransduced *Hoxc4*$^{+/+}$ and *Hoxc4*$^{-/-}$ B cells, CSR was greatly reduced in *Hoxc4*$^{-/-}$ B cells transduced with the TAC control retrovirus as compared to theirs transduced *Hoxc4*$^{+/+}$ counterparts (Fig. 9a,b). In *Hoxc4*$^{+/+}$ B cells, enforced expression of AID increased CSR to IgG1 by about 50%. TAC-*Aicda* retrovirus-transduction of *Hoxc4*$^{-/-}$ B cells increased *Aicda* expression. It did not modulate the expression of germline I_μ-C_μ and $I_\gamma1$-$C_\gamma1$ transcripts, but increased CSR to IgG1 to a level comparable to that of TAC-*Aicda* retrovirus-transduced *Hoxc4*$^{+/+}$ B cells, as shown by the increased proportion of surface IgG$^+$ B cells and more circle $I_\gamma1$-C_μ and post-recombination I_μ-$C_\gamma1$ transcripts. These experiments show that defective AID expression and CSR in *Hoxc4*$^{-/-}$ B cells are rescued by enforced AID expression further indicating that HoxC4 modulates CSR by regulating AID expression.

DISCUSSION

In B cells, AID expression is tightly regulated31–34, possibly in an activation-dependent manner in conditions under which CSR and SHM unfold. The specificity and the level of AID expression are likely controlled by a complex combination of different tissue specific transcription factors, both activators and repressors. Here we have provided evidence that by binding to the highly conserved 5'-ATTTGAAT-3' motif in the *Aicda* promoter, HoxC4 activates this promoter, thereby modulating AID expression, CSR and SHM. In this function, HoxC4 synergizes with Oct1–Oct2, which also binds to the 5'-ATTTGAAT-3' motif, in a fashion similar to that we reported for the HoxC4-Oct-mediated activation of the human 3'E_α hs1,2 enhancer element25. Accordingly, *Hoxc4*$^{-/-}$ mice or B cells display defective CSR and SHM, despite normal levels of mature V_HDJ_H and germline I_H-C_H transcripts31. The efficient rescue of CSR by enforced expression of AID in *Hoxc4*$^{-/-}$ B cells indicates that induction of AID is the major pathway through which HoxC4 regulates CSR and, likely, SHM. Mutation of the 5'-ATTTGAAT-3' site to 5'-gcTTGAATT-3', which did not disrupt Oct-binding and introduced a putative Sp site, did not seemingly alter *Aicda* promoter activity in mouse B-lymphoma M12 and CH33 and human embryonic kidney

fibroblast 293 cells16. In our experiments, mutation of 5'-ATTTGAAT-3' to disrupt HoxC4-binding, while preserving the Oct-binding activity, or to abrogate the binding of Oct1–Oct2 but not that of HoxC425, reduced *Aicda* transcription, thereby highlighting the role of these homeodomain transcription factors in AID expression and adding another dimension to the function of Oct1–Oct2 in B cell differentiation.

As we have shown in human B cells, HoxC4 plays an important and complex role in the regulation of the IgH locus24,25,35. The putatively dampening effect of HoxC4 on the baseline activity of the I_γ and I_ε promoters would be effectively lifted and overridden by the strong activation of these promoters by CD40-signaling and CD154-induced HoxC4-mediated activation of the hs1,2 enhancer element24,25,35. The role of HoxC4 in the induction of AID expression is further strengthened by our demonstration that, like AID, HoxC4 is preferentially expressed in GC B cells of both humans24 and mice (these results), and CD154:CD40 engagement and cytokines, which induce the expression of *AICDA* and *Aicda*, also induce *HOXC4* and *Hoxc4* in human24 and mouse B cells, respectively (these results). Further, NF-κB-binding sites in both the human and mouse *HOXC4* and *Hoxc4* promoters underpin the upregulation of HoxC4 by CD40 signaling.

Consistent with the notion that the defect in CSR and SHM manifested by *Hoxc4*$^{-/-}$ B cells was due to a failure to induce *Aicda* expression, both *Aicda* transcripts and AID protein, as induced by LPS and IL-4 or CD154 and IL-4, were significantly decreased in *Hoxc4*$^{-/-}$ B cells. The tissue- and differentiation stage-specificity of HoxC4 expression would account to a great extent for the precise regulation of AID expression. In *Hoxc4*$^{-/-}$ mice, the decreased AID expression was reflected *in vivo* into the impairment of the maturation of the T-dependent antibody response. In these mice, although *Aicda* expression was significantly reduced, GC formation was seemingly normal. This is reminiscent of *Aicda*$^{+/-}$ mice36, which also show normal GCs in the presence of significantly decreased *Aicda* expression37,38 and contrasts with *Aicda*$^{-/-}$ mice, in which activated B cells accumulate and form giant GCs36.

The B cell lineage-specific Pax5 transcription factor has been suggested to play a role in *Aicda* expression by binding to the 5'-GGGGAGGAGCC-3' site in the *Aicda* promoter16. This *cis*-element, however, does not fulfill the requirements of a consensus Pax5-binding motif and did not bind Pax5 in our experiments and those by others17. Our finding on the lack of specificity of the conserved 5'-GGGGAGGAGCC-3' *cis*-element for Pax5 suggests that the recruitment of Pax5 to the *Aicda* promoter, as revealed by ChIP assays, occurred indirectly, through other DNA-binding transcription factors, perhaps, Sp1 or Sp3, in a fashion similar to the interaction between estrogen receptor and Sp1 on certain estrogen-responsive promoters39.

The B cell development-related E47 transcription factor has been suggested to contribute to the enhancement of the *Aicda* promoter activity by binding to E-boxes in the *cr2* of the first intron of this gene21,22. E47-induced enhancement of the *Aicda* promoter activity would be modulated by the E2A inhibitor Id315. The presence of *cr2* in human Ramos and mouse CH12F3-2A B cells (our findings), and in mouse BaF/3 pro-B cells or M12 B cells16 did not enhance luciferase reporter transcription, as driven by the *Aicda* promoter. This might

reflect the dispensability of E2A transcription factors in *AICDA* and *Aicda* expression, CSR, and possibly, SHM, as shown by analysis of E2A-deficient B cells40,41, or a muted baseline activity of *cr2*, resulting from a preferential binding of Id2 and/or Id3 to this region. These experiments, however, cannot rule out the possibility that, like the IgH and Igκ intronic enhancers, which contain multiple E-box sites and show a high enhancer activity in GC B cells42, *cr2* and E-proteins act together with HoxC4 to synergistically induce AID expression.

The HoxC4-mediated *Aicda* promoter activation is further enhanced by the upstream conserved 5'-GGGGAGGAGCC-3' site, which, as we have also shown, recruits Sp1, Sp3 and NF-κB. Sp1 and Sp3 bind directly to DNA through their zinc finger motifs and enhance gene transcription. These proteins are ubiquitously expressed and are directly involved not only in the regulation of basal transcription and expression of housekeeping genes, but also in developmentally controlled gene expression. In our experiments, the Sp-NF-κB site could partially mediate *Aicda* promoter activity in the absence of the HoxC4-Oct1–Oct2 site, and possibly accounted for the residual AID expression, CSR and SHM in *Hoxc4*$^{-/-}$ B cells and mice.

We showed that OcaB was also recruited to the *AICDA* and *Aicda* promoters in B cells undergoing CSR or SHM, likely through interaction with Oct1–Oct243. By clamping the Oct1–Oct2 POU_H and POU_S subdomains, OcaB would increase the affinity of these homeodomain proteins for DNA, thereby potentiating HoxC4- and Oct1–Oct2-mediated *Aicda* promoter activation. As we have shown, OcaB plays an important role in HoxC4 and Oct1–Oct2-mediated activation of the human 3'Eα enhancer hs1,2 element25. Accordingly, mice lacking OcaB show an impairment in CSR43. The present experiments unveil another role for Oct1–Oct2 and OcaB activity: the regulation of AID expression. Overall, our findings offer fundamental insights into the mechanisms of activation of the *AICDA* and *Aicda* promotera and induction of AID expression, CSR and SHM. The possibility that the induction of HoxC4 by stimuli other than CD40-signaling, LPS and cytokines, such as hormone (our unpublished data), modulates AID expression and, therefore, antibody diversification in health and disease should be addressed.

METHODS

Hoxc4$^{-/-}$ mice

In these *Hoxc4*$^{-/-}$ mice (A.M. Boulet and M.R. Capecchi, HHMI, University of Utah, Salt Lake City, UT), *Hoxc4* was disrupted through insertion of a *lox*P site in exon 2 of this gene at the coding sequence for the amino-terminal end (between the third and the fourth codons) of the homeobox, which introduces a stop codon at the insertion site, yielding a nonfunctional truncated protein (lacking 95% of the homeodomain) (unpublished findings). We obtained this *Hoxc4*$^{+/-}$ frozen sperm and re-derived *Hoxc4*$^{+/-}$ mice by *in vitro* fertilization through the services of the UC Irvine transgenic mouse facility. These *Hoxc4*$^{+/-}$ mice are in the C57BL/6 background after backcrossing the 129Sv/Ev founder strain with C57BL/6 mice. *Hoxc4*$^{-/-}$ mice and their WT littermates have been bred under pathogen-free conditions. The Institutional Animal Care and Use Committee (IACUC) of University of California, Irvine, CA, approved all animal experiments.

B and T cells

The number of B cells ($B220^+$) and T cells ($CD3^+$), the proportion $CD4^+$ T cells, dead B and T cells and the proportion of PNA^{hi} B cells, plasma cells ($B220^{lo}$ $CD138^+$) and NP-binding $CD38^{hi}$ $IgG1^+$memory B cells were determined by FACS analysis using a FACSCalibur ™ flow cytometer (BD Biosciences). Single cell suspensions were prepared from spleens or Peyer's patches of *Hoxc4*$^{-/-}$ and *Hoxc4*$^{+/+}$ mice and stained with Phycoerythrin (PE)-labeled anti-mouse B220 mAb (clone RA3-6B2) (eBioscience Corp.), fluorescein isothiocyanate (FITC)-labeled anti-mouse CD3 mAb (clone 17A2) (BioLegend, Inc.), PerCP-anti-mouse CD4 mAb (clone GK1.5) (BioLegend, Inc.), 7-AAD (BD Biosciences), FITC-PNA, FITC-anti-mouse CD138 mAb (clone 281-2) or APC-anti-mouse IgG1 (clone X56) (BD Biosciences), PE-NP (Biosearch Technologies, Inc.) and PECy7-anti-mouse CD38 mAb (clone 90) (eBiosciences Corp.). Single $B220^+$ cell suspensions were prepared from spleens or Peyer's patches using the EasySep® Mouse B Cell Enrichment Kit (StemCell Technologies Inc.). For the preparation of PNA^{hi} (GC) B cells, spleen or Peyer's patches B cells were stained with PE-anti-mouse CD45R (B220) mAb (clone RA3-6B2) (BD Biosciences) and FITC-PNA. Labeled lymphocytes were then sorted using a MoFlow™ cell sorter (Dako), yielding 95% pure PNA^{hi} $B220^+$ cells.

B cell lines

Ramos B cells were monitored for spontaneous SHM44. Monoclonal 4B6 and 2E2 B cell lines were derived from our CSR- and SHM-inducible human monoclonal IgM^+IgD^+ CL-01 B cell line45–50 by sequential subcloning and selection for spontaneous and inducible CSR, respectively. 4B6 B cells are IgM^+IgD^+ with an "early" GC phenotype and undergo spontaneous CSR to IgG, IgE, and IgA24. 2E2 B cells are IgM^+IgD^+ and undergo CSR to IgG, IgE, and IgA upon stimulation by an agonistic anti-huCD40 mAb and appropriate cytokines51. The mouse B lymphoma cell line CH12F3-2A was obtained from T. Honjo (Kyoto University, Japan). CH12F3-2A cells are surface IgM^+ and switch to IgA upon the stimulation with CD154 or LPS in the presence of IL-4 and TGF-β152. All these monoclonal B cells were cultured in RPMI 1640 medium (Invitrogen Corp.) supplemented with 10% heat-inactivated fetal bovine serum (Hyclone), 2 mM L-glutamine, and 1x antibiotic-antimycotic mixture (100 units/ml penicillin, 100 mg/ml streptomycin, 0.25 mg/ml amphotericin B fungizone) (Invitrogen Corp.) (FBS-RPMI).

B cell cycle and proliferation

Cell cycle was analyzed by PI staining50. Proliferation was analyzed using the CellTrace™ CFSE Cell Proliferation Kit (Molecular Probes Co.). Cells were washed in serum-free HBSS (Invitrogen Corp.) and resuspended at 1×10^6 cells/ml. After adding an equal volume of 2.4 mM CFSE, cells were incubated at 37 °C for 12 min and then washed in FBS-RPMI. Cells were then diluted and cultured in the presence or absence of LPS (20 μg/ml) from *E. coli* (serotype 055:B5) (Sigma-Aldrich Co.) and recombinant mouse (rmo)IL-4 (5 ng/ml; R&D Systems, Inc.), harvested at various time points after activation and analyzed by FACS. For *in vivo* B cell proliferation, mice were immunized with NP_{16}-CGG. After 10 d, they were injected intraperitoneally twice within 16 h with BrdU (1 mg) and sacrificed 4 h after the last injection. Cells from the spleen or Peyer's patches were stained with PE-anti-mouse

B220 mAb (BD Biosciences) or this mAb together with FITC-PNA. Incorporated BrdU was stained with APC-anti-BrdU mAb using APC BrdU Flow Kit (BD Biosciences) and analyzed by FACS.

Analysis of *in vitro* CSR

Enriched spleen B cells were cultured at 1×10^6 cell/ml in FBS-RPMI with 0.05 mM β-mercaptoethanol. Cells were stimulated with LPS (20 μg/ml) or CD154-expressing membrane fragments of baculovirus-infected Sf21 insect cells (referred to CD154)53 and: with (i) nil for CSR to IgG3 and IgG2b; (ii) rmIL-4 (5 ng/ml) for CSR to IgG1 and IgE; (iii) IFN-γ (50 ng/ml; PeproTech Inc.) for CSR to IgG2a; and (iv) TGF-β1 (1 ng/ml; R&D Systems, Inc.), rmIL-5 (5 ng/ml; R&D Systems, Inc.), and anti-δmAb-dextran (3 ng/ml; provided by C. M. Snapper, Uniformed Services University of the Health Sciences, Bethesda, MD) for CSR to IgA. Cells were collected on day 4 for surface Ig analysis, after staining with FITC-anti-mouse IgG1 (clone A85-1), anti-mouse IgG2a (clone R19-15), anti-mouse IgG2b (clone R12-3) anti-mouse IgG3 (clone R40-82) or anti-mouse IgA (clone C10-3) rat mAb and PE-anti-mouse CD45R (B220) (clone RA3-6B2) rat mAb (BD Biosciences). Cells were fixed with 1% paraformaldehyde in PBS and analyzed by FACS. Specific ELISAs involving 96 well plates coated with polyclonal goat Ab $F(ab)_2$ against the respective mouse isotype (SouthernBiotechnology Associates, Inc.) were used to measure IgG1, IgG2a, IgG2b, IgG3, IgA and IgE in culture supernatants of *in vitro* stimulated spleen *Hoxc4*$^{+/+}$ and *Hoxc4*$^{-/-}$ B cells. Supernatants were serially twofold diluted from 1:5 to 1:640, and then added (100 μl per well) to the 96-well plates. Plates were incubated for 1 h at 25°C. After washing, biotin-labeled isotype-specific mAbs were added and then revealed using HRP-streptavidin, as described above. The concentration of the different Ig isotypes was determined by interpolation using a calibrated standard curve for each isotype. The assays were performed in triplicates.

Quantitative real-time RT-PCR (qRT-PCR) and semiquantitative RT-PCR

RNA was extracted using the RNeasy Mini Kit (Qiagen Inc.) according to the manufacturer's protocol. Residual DNA was removed by treatment with DNase I (Invitrogen Corp.). First strand cDNAs were synthesized from equal amounts of total RNA (2 μg) using the SuperScript™ Preamplification System and oligo (dT) primer (Invitrogen Corp.). The expression of germline I_H-C_H, post-recombination I_μ-C_H, mature $V_{J558}DJ_H$-C_μ, *Hoxc4* and *Aicda* transcripts was quantified by real-time qRT-PCR54 using appropriate primers (Operon Corp.) (Supplementary Table 1 online). In some cases, circle $I_\gamma 1$-C_μ transcripts, *HOXC4*, *Hoxc4*, *AICDA* and *Aicda* transcripts were analyzed by specific semiquantitative RT-PCR by performing serial twofold dilutions so that there was a virtually linear relationship between the amount of cDNA used and the intensity of the PCR product. Real-time qRT-PCR analysis was performed using an DNA Engine Opticon 2 Real-Time PCR Detection System (Bio-Rad Laboratories, Inc.) to measure SYBR-green (DyNAmo HS SYBR Green, New England Biolabs, Inc.) incorporation with the following protocol: 50 °C for 2 min, 95 °C for 10 min, 40 cycles of 95 °C for 10 sec, 60 °C for 20 sec, 72 °C for 30 sec, 80 °C for 1 sec, and data acquisition at 80 °C, and 72 °C for 10 min. Melting curve analysis was performed from 72°–95 °C and samples were incubated for another 5 min at 72 °C. The ΔΔCt method was used for data analysis.

Analysis of somatic mutations in intronic J_H4-iE_μ DNA

Peyer's patch B cells were obtained from non-intentionally immunized 12-week-old littermate *Hoxc4*$^{-/-}$ and *Hoxc4*$^{+/+}$ C57BL/6 mice and used to analyze somatic-mutations in the intronic DNA downstream of rearranged $V_{J558}DJ_H4$ genes. Platinum® Pfx DNA polymerase (Invitrogen Corp.) was utilized for genomic DNA amplifications. The intronic IgH region downstream of rearranged $V_{J558}DJ_H$ was amplified using nested PCR55 involving two V_H J558 framework region (FR)3-specific forward primers, and two reverse primers specific for sequences downstream of J_H4 (Supplementary Table 1).yielding an approximately 900 bp DNA if a J_H4 rearrangement occurred. PCR conditions were 94°C for 45 sec, 58°C for 45 sec, 68°C for 1 min for 35 cycles. PCR products were cloned into the pCR-Blunt II-TOPO® vector (Invitrogen Corp.) and sequenced. Only sequences from rearrangements involving J_H4-iEμ were analyzed. Sequences were analyzed using the MacVector™ 7.2.3 software (MacVector, Inc.).

Identification of putative transcription factor-binding sites

The putative transcription factor binding sites in the AID gene promoter sequence were identified by weight matrix search using Match™ (http://www.gene-regulation.com/cgi-bin/pub/programs/match/bin/match.cgi) (BIOBASE Corp.) which integrates TRANSFAC® 6.0 and uses its positional weight matrices for analysis. Scores indicate the degree of fitness of the putative binding site with the consensus sequence: score 1.0 = 100%; the cut-off score used was 0.75.

Aicda promoter luciferase gene reporter assays

The reporter constructs were consisted of the pGL3-Basic (experiments of Fig. 6d) or pGL3-Enhancer (experiments of Fig. 8a) Firefly luciferase gene reporter vector (Promega Corp.) and different *Aicda* locus DNA sequences. An 839-bp 5'*R-AID-Pro*, 490 bp 5'*R* or 349 bp *AID-Pro* sequences and first intron conserved regions (*cr1* and *cr2*) were amplified by PCR from C57BL/6 mouse genomic DNA, and were inserted in upstream and/or downstream of the luciferase gene in pGL3 vector. Various mutant reporters were constructed by QuikChange™ Site-Directed Mutagenesis (Stratagene). Sequences of constructs were confirmed by at least two sequencing reactions. Co-transfection of the reporter construct and the constitutively active *Renilla reniformis* luciferase producing vector pRL-TK (Promega, Corp.) in human Ramos, 4B6 and mouse CH12F3-2A B cells was performed by electroporation24, 25, 35. Firefly and *Renilla reniformis* luciferase activities were measured using the Dual-Luciferase® Reporter Assay System (Promega, Corp.) according to manufacturer's instructions.

Chromatin immunoprecipitation assays (ChIP)

B cells (5×10^7) were treated with 1% formaldehyde for 10 min at 25 °C to cross-link chromatin. After washing with cold PBS containing protease inhibitors (Roche, Basel, Switzerland), chromatin was separated using nuclear lysis buffer (10 mM Tris-HCl, 1 mM EDTA, 0.5 M NaCl, 1% Triton-X-100, 0.5% sodium deoxycholate, 0.5% Sarcosyl, pH 8.0) and resuspended in IP-1 buffer (20 mM Tris-HCl, pH 8.0 200 mM NaCl, 2 mM EDTA, 0.1% sodium deoxycholate, 0.1% SDS, protease inhibitors). Chromatin was sonicated to

yield approximately 200–1000 bp DNA fragments, precleared with agarose beads bearing protein G (Santa Cruz Biotechnology, Inc.) and then incubated with mouse mAbs to HoxC4, or rabbit polyclonal Abs to Oct1, Oct2, OcaB, Pax5, Sp1, Sp3, or NF-κB (p52 subunit) at 4 °C. After overnight incubation, immune complexes were isolated using agarose-beads bearing protein G, eluted with Elution buffer (50 mM Tris-HCl, 0.5% SDS, 200 mM NaCl, 100 μg/ml Proteinase K, pH 8.0), and then incubated at 65 °C overnight to reverse formaldehyde cross-links. DNA was extracted by phenol/chloroform and precipitated by ethanol, and then resuspended in TE buffer (10 mM Tris-HCl, pH 8.0, 1 mM EDTA). DNA sequences were specified by PCR using appropriate primers (Supplementary Table 1 online).

Retroviral transduction of B cells

The TAC and TAC-*Aicda* retroviral constructs15 containing the human *IL2RA* gene encoding CD25 (TAC antigen) or this gene together with the mouse *Aicda* coding sequence were obtained from C. Murre (University of California, San Diego). To generate retrovirus, the pCSretTAC-based constructs were transfected into the HEK-293T packaging cell line, using ProFection® Mammalian Transfection System (Promega Corp.). The retroviral constructs were used to transduce mouse spleen B cells as reported15.

Statistical analyses

The differences in frequency and spectrum of mutations in $Hoxc4^{-/-}$ and $Hoxc4^{+/+}$ mice were analyzed using the χ^2 test. The differences in Ig titers, CSR or mRNA expression were analyzed using paired *t*-tests.

Supplementary Material

Refer to Web version on PubMed Central for supplementary material.

ACKNOWLEDGEMENTS

We thank M.R. Capecchi and A.M. Boulet for kindly providing us with the $Hoxc4^{+/-}$ mouse frozen sperm, T. Fielder for re-deriving $Hoxc4^{+/-}$ mice, C.M. Snapper for the anti-δ-mAb-dextran, C. Murre for the *Aicda* retroviral construct, T. Honjo for CH12F3-2A cells and Z. Yu for statistic analysis. We are also grateful to A. Schaffer for discussion, S. Sabet and M. Kang for excellent technical assistance. This work was supported by NIH grants AI 045011, AI 079705 and AI 060573 to P.C., and Korea Research Foundation grant KRF-2005-214-C00131 to S.-R. P.

REFERENCES

1. Honjo T, Kinoshita K, Muramatsu M. Molecular mechanism of class switch recombination: linkage with somatic hypermutation. Annu. Rev. Immunol. 2002; 20:165–196. [PubMed: 11861601]
2. Honjo T, Muramatsu M, Fagarasan S. Aid: How does it aid antibody diversity? Immunity. 2004; 20:659–668. [PubMed: 15189732]
3. Neuberger MS, Harris RS, Di Noia J, Petersen-Mahrt SK. Immunity through DNA deamination. Trends Biochem. Sci. 2003; 28:305–312. [PubMed: 12826402]
4. Chaudhuri J, Alt FW. Class-switch recombination: interplay of transcription, DNA deamination and DNA repair. Nat. Rev. Immunol. 2004; 4:541–552. [PubMed: 15229473]

5. Rada C, Di Noia JM, Neuberger MS. Mismatch recognition and uracil excision provide complementary paths to both Ig switching and the A/T-focused phase of somatic mutation. Mol. Cell. 2004; 16:163–171. [PubMed: 15494304]
6. Maizels N. Immunoglobulin gene diversification. Annu. Rev. Genet. 2005; 39:23–46. [PubMed: 16285851]
7. Di Noia JM, Neuberger MS. Molecular mechanisms of antibody somatic hypermutation. Annu. Rev. Biochem. 2007; 76:1–22. [PubMed: 17328676]
8. Peled JU, et al. The biochemistry of somatic hypermutation. Annu. Rev. Immunol. 2008; 26:481–511. [PubMed: 18304001]
9. Diaz M, Casali P. Somatic immunoglobulin hypermutation. Curr. Opin. Immunol. 2002; 14:235–240. [PubMed: 11869898]
10. Papavasiliou FN, Schatz DG. Somatic hypermutation of immunoglobulin genes; merging mechanisms for genetic diversity. Cell. 2002; 109:s35–s44. [PubMed: 11983151]
11. Wu X, et al. Immunoglobulin somatic hypermutation: double-strand DNA breaks, AID and error-prone DNA repair. J. Clin. Immunol. 2003; 23:235–246. [PubMed: 12959216]
12. Xu Z, et al. DNA lesions and repair in immunoglobulin class switch recombination and somatic hypermutation. Ann. N.Y. Acad. Sci. 2005; 1050:146–162. [PubMed: 16014529]
13. Casali P, Pal Z, Xu Z, Zan H. DNA repair in antibody somatic hypermutation. Trends Immunol. 2006; 27:313–321. [PubMed: 16737852]
14. Yan CT, et al. IgH class switching and translocations use a robust non-classical end-joining pathway. Nature. 2007; 449:478–482. [PubMed: 17713479]
15. Sayegh CE, Quong MW, Agata Y, Murre C. E-proteins directly regulate expression of activation-induced deaminase in mature B cells. Nat. Immunol. 2003; 4:586–593. [PubMed: 12717431]
16. Gonda H, et al. The balance between Pax5 and Id2 activities is the key to AID gene expression. J. Exp. Med. 2003; 198:1427–1437. [PubMed: 14581609]
17. Yadav A, et al. Identification of a ubiquitously active promoter of the murine activation-induced cytidine deaminase (AICDA) gene. Mol. Immunol. 2006; 43:529–541. [PubMed: 16005067]
18. Pearson JC, Lemons D, McGinnis W. Modulating Hox gene functions during animal body patterning. Nat. Rev. Genet. 2005; 6:839–904.
19. Zakany J, Duboule D. The role of Hox genes during vertebrate limb development. Curr. Opin. Genet. Dev. 2007; 17:359–366. [PubMed: 17644373]
20. Deschamps J, van Nes J. Developmental regulation of the Hox genes during axial morphogenesis in the mouse. Development. 2005; 132:2931–2942. [PubMed: 15944185]
21. Lemons D, McGinnis W. Genomic evolution of Hox gene clusters. Science. 2006; 313:1918–1922. [PubMed: 17008523]
22. Bijl J, et al. Expression of HOXC4, HOXC5, and HOXC6 in human lymphoid cell lines, leukemias, and benign and malignant lymphoid tissue. Blood. 1996; 87:1737–1745. [PubMed: 8634419]
23. Meazza R, et al. Expression of HOXC4 homeoprotein in the nucleus of activated human lymphocytes. Blood. 1995; 85:2084–2090. [PubMed: 7718879]
24. Schaffer A, et al. Selective inhibition of class switching to IgG and IgE by recruitment of the HoxC4 and Oct-1 homeodomain proteins and Ku70/Ku86 to newly identified ATTT cis-elements. J. Biol. Chem. 2003; 278:23141–23150. [PubMed: 12672812]
25. Kim EC, Edmonston CR, Wu X, Schaffer A, Casali P. The HoxC4 homeodomain protein mediates activation of the immunoglobulin heavy chain 3' hs1,2 enhancer in human B cells. Relevance to class switch DNA recombination. J. Biol. Chem. 2004; 279:42258–42269. [PubMed: 15252056]
26. Pasqualucci L, et al. Expression of the AID protein in normal and neoplastic B cells. Blood. 2004; 104:3318–3325. [PubMed: 15304391]
27. Guikema JE, et al. Quantitative RT-PCR analysis of activation-induced cytidine deaminase expression in tissue samples from mantle cell lymphoma and B-cell chronic lymphocytic leukemia patients. Blood. 2005; 105:2997–2998. [PubMed: 15781912]

28. Bijl JJ, et al. HOXC4, HOXC5, and HOXC6 expression in non-Hodgkin's lymphoma: preferential expression of the HOXC5 gene in primary cutaneous anaplastic T-cell and oro-gastrointestinal tract mucosa-associated B-cell lymphomas. Blood. 1997; 90:4116–4125. [PubMed: 9354682]
29. Boulet AM, Capecchi MR. Targeted disruption of hoxc-4 causes esophageal defects and vertebral transformations. Dev. Biol. 1996; 177:232–249. [PubMed: 8660891]
30. Saegusa H, Takahashi N, Noguchi S, Suemori H. Targeted disruption in the mouse Hoxc-4 locus results in axial skeleton homeosis and malformation of the xiphoid process. Dev. Biol. 1996; 174:55–64. [PubMed: 8626021]
31. Xu Z, et al. Regulation of aicda expression and AID activity: relevance to somatic hypermutation and class switch DNA recombination. Crit. Rev. Immunol. 2007; 27:367–397. [PubMed: 18197815]
32. Crouch EE, et al. Regulation of AID expression in the immune response. J. Exp. Med. 2007; 204:1145–1156. [PubMed: 17452520]
33. Teng G, et al. MicroRNA-155 is a negative regulator of activation-induced cytidine deaminase. Immunity. 2008; 28:621–629. [PubMed: 18450484]
34. Dedeoglu F, Horwitz B, Chaudhuri J, Alt FW, Geha RS. Induction of activation-induced cytidine deaminase gene expression by IL-4 and CD40 ligation is dependent on STAT6 and NFkappaB. Int. Immunol. 2004; 16:395–404. [PubMed: 14978013]
35. Schaffer A, Cerutti A, Shah S, Zan H, Casali P. The evolutionary conserved sequence upstream of the human Ig Sγ3 region is an inducible promoter: Synergistic activation by CD40 ligand and IL-4 via cooperative NF-κB and STAT-6 binding sites. J. Immunol. 1999; 162:5327–5336. [PubMed: 10228008]
36. Muramatsu M, et al. Class switch recombination and hypermutation require activation-induced cytidine deaminase (AID), a potential RNA editing enzyme. Cell. 2000; 102:553–563. [PubMed: 11007474]
37. Jiang C, Zhao ML, Diaz M. Activation-induced deaminase heterozygous MRL/lpr mice are delayed in the production of high-affinity pathogenic antibodies and in the development of lupus nephritis. Immunology. 2008; 126:102–113. [PubMed: 18624728]
38. Takizawa M, et al. AID expression levels determine the extent of cMyc oncogenic translocations and the incidence of B cell tumor development. J. Exp. Med. 2008; 205:1949–1957. [PubMed: 18678733]
39. Saville B, et al. Ligand-, cell-, and estrogen receptor subtype (alpha/beta)-dependent activation at GC-rich (Sp1) promoter elements. J. Biol. Chem. 2000; 275:5379–5387. [PubMed: 10681512]
40. Kwon K, et al. Instructive role of the transcription factor E2A in early B lymphopoiesis and germinal center B cell development. Immunity. 2008; 28:751–762. [PubMed: 18538592]
41. Schoetz U, Cervelli M, Wang Y-D, Fiedler P, Buerstedde J-M. E2A expression stimulates Ig hypermutation. J. Immunol. 2006; 177:395–400. [PubMed: 16785535]
42. Odegard VH, Kim ST, Anderson SM, Shlomchik MJ, Schatz DG. Histone modifications associated with somatic hypermutation. Immunity. 2005; 23:101–110. [PubMed: 16039583]
43. Teitell MA. OCA-B regulation of B-cell development and function. Trends Immunol. 2003; 24:546–553. [PubMed: 14552839]
44. Sale JE, Neuberger MS. TdT-accessibe breaks are scattered over the immunoglobulin V domain in a constitutively hypermutating B cell line. Immunity. 1998; 9:859–869. [PubMed: 9881976]
45. Cerutti A, et al. CD40 ligand and appropriate cytokines induce switching to IgG, IgA, and IgE and coordinated germinal center and plasmacytoid phenotypic differentiation in a human monoclonal IgM^+IgD^+ B cell line. J. Immunol. 1998; 160:2145–2157. [PubMed: 9498752]
46. Zan H, et al. Induction of Ig somatic hypermutation and class switching in a human monoclonal IgM^+ IgD^+ cell line in vitro: Definition of the requirements and the modalities of hypermutation. J. Immunol. 1999; 162:3437–3447. [PubMed: 10092799]
47. Zan H, Cerutti A, Schaffer A, Dramitinos P, Casali P. CD40 engagement triggers switching to IgA1 and IgA2 in human B cells through induction of endogenous TGF-β. Evidence for TGF-β but not IL-10-dependent direct Sμ→Sα and sequential Sμ→Sγ, Sγ→Sα DNA recombination. J. Immunol. 1998; 161:5217–5225. [PubMed: 9820493]

48. Zan H, et al. The translesion DNA polymerase ζ plays a major role in Ig and Bcl-6 somatic hypermutation. Immunity. 2001; 14:643–653. [PubMed: 11371365]
49. Zan H, et al. BCR engagement and T cell contact induce *Bcl-6* hypermutation in human B cells: association with initiation of transcription and identity with Ig hypermutation. J. Immunol. 2000; 165:830–839. [PubMed: 10878357]
50. Zan H, Wu X, Komori A, Holloman WK, Casali P. AID-dependent generation of resected double-strand DNA breaks and recruitment of Rad52/Rad51 in somatic hypermutation. Immunity. 2003; 18:727–738. [PubMed: 12818155]
51. Zan H, Casali P. AID- and Ung-dependent generation of staggered double-strand DNA braeks in immunoglobulin class switch DNA recombination: A post-cleavage role for AID. Mol. Immunol. 2008; 46:45–61. [PubMed: 18760480]
52. Muramatsu M, et al. Specific expression of activation-induced cytidine deaminase (AID), a novel member of the RNA-editing deaminase family in germinal center B cells. J. Biol. Chem. 1999; 274:18470–18476. [PubMed: 10373455]
53. Rush JS, Liu M, Odegard VH, Unniraman S, Schatz DG. Expression of activation-induced cytidine deaminase is regulated by cell division, providing a mechanistic basis for division-linked class switch recombination. Proc. Natl. Acad. Sci. U.S.A. 2005; 102:13242–13247. [PubMed: 16141332]
54. Zan H, et al. Lupus-prone MRL/faslpr/lpr mice display increased AID expression and extensive DNA lesions, comprising deletions and insertions, in the immunoglobulin locus: Concurrent upregulation of somatic hypermutation and class switch DNA recombination. Autoimmunity. 2009; 42:89–103. [PubMed: 19156553]
55. Zan H, et al. The translesion DNA polymerase θ plays a major role in immunoglobulin gene somatic hypermutation. EMBO J. 2005; 24:3757–3769. [PubMed: 16222339]

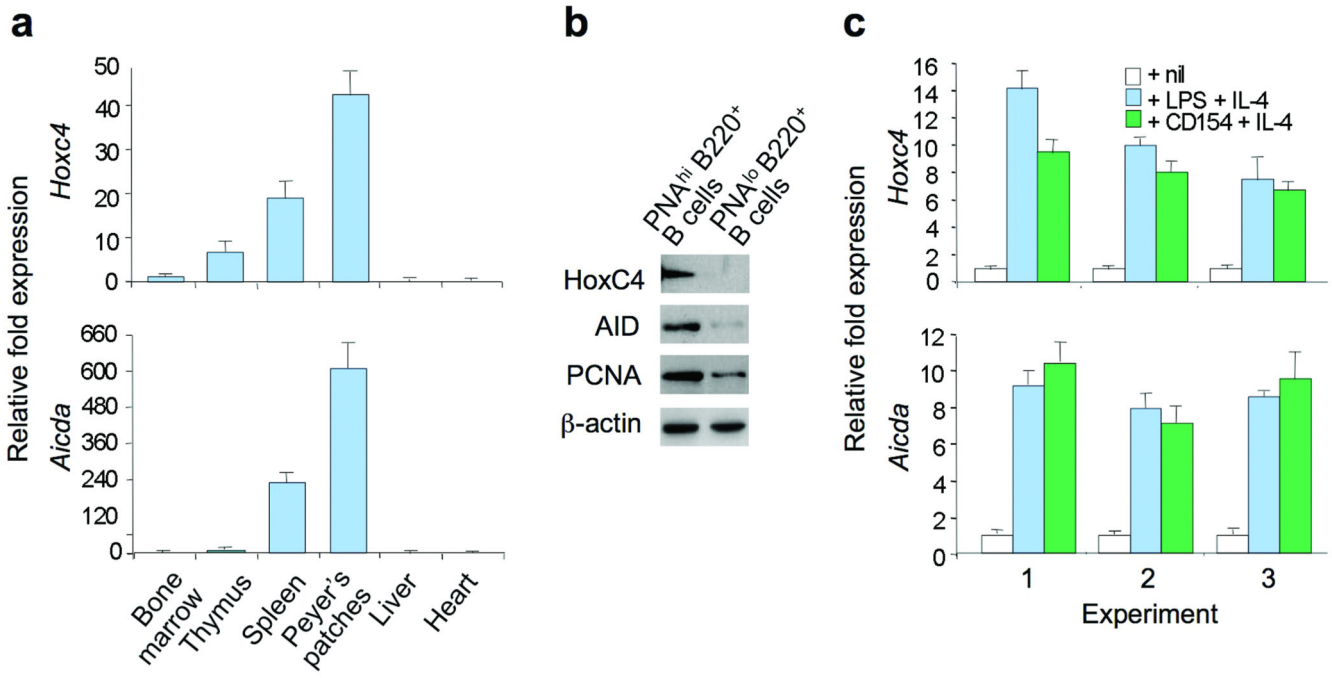

Figure 1.

Hoxc4 expression correlates with *Aicda* expression. (**a**) *Hoxc4* and *Aicda* transcripts in bone marrow, thymus, spleen, Peyer's patches, liver or heart of C57BL/6 mice, as measured by real-time qRT-PCR performed in triplicate samples using SYBR-green. In each sample, mRNA expression was normalized to *Gapdh* expression. Data are means ± s.e. (bars) of fold mRNA in the indicated tissue compared to bone marrow of 3 independent experiments. (**b**) HoxC4, AID, PCNA and β-actin protein expression in $PNA^{hi}B220^{+}$ (GC) B cells and $PNA^{lo}B220^{+}$ (non-GC) B cells from spleen of NP_{16}-CGG immunized mice, as detected by immunoblotting. Data are from 2 independent experiments. (**c**) Increased expression of *Hoxc4* and *Aicda* mRNA in LPS and IL-4- or CD154 and IL-4-stimulated spleen B cells, as determined by real-time qRT-PCR. Spleen B cells from 3 C57BL/6 mice were cultured with nil, LPS plus IL-4 or CD154 plus IL-4, and harvested after 3 d to extract RNA and perform real-time qRT-PCR. mRNA expression was normalized to *CD79b* transcripts. Data are from 3 independent experiments. In each experiment, values are means ± s.e. (bars) of fold mRNA levels in B cells stimulated as indicated, as compared to unstimulated B cells (nil).

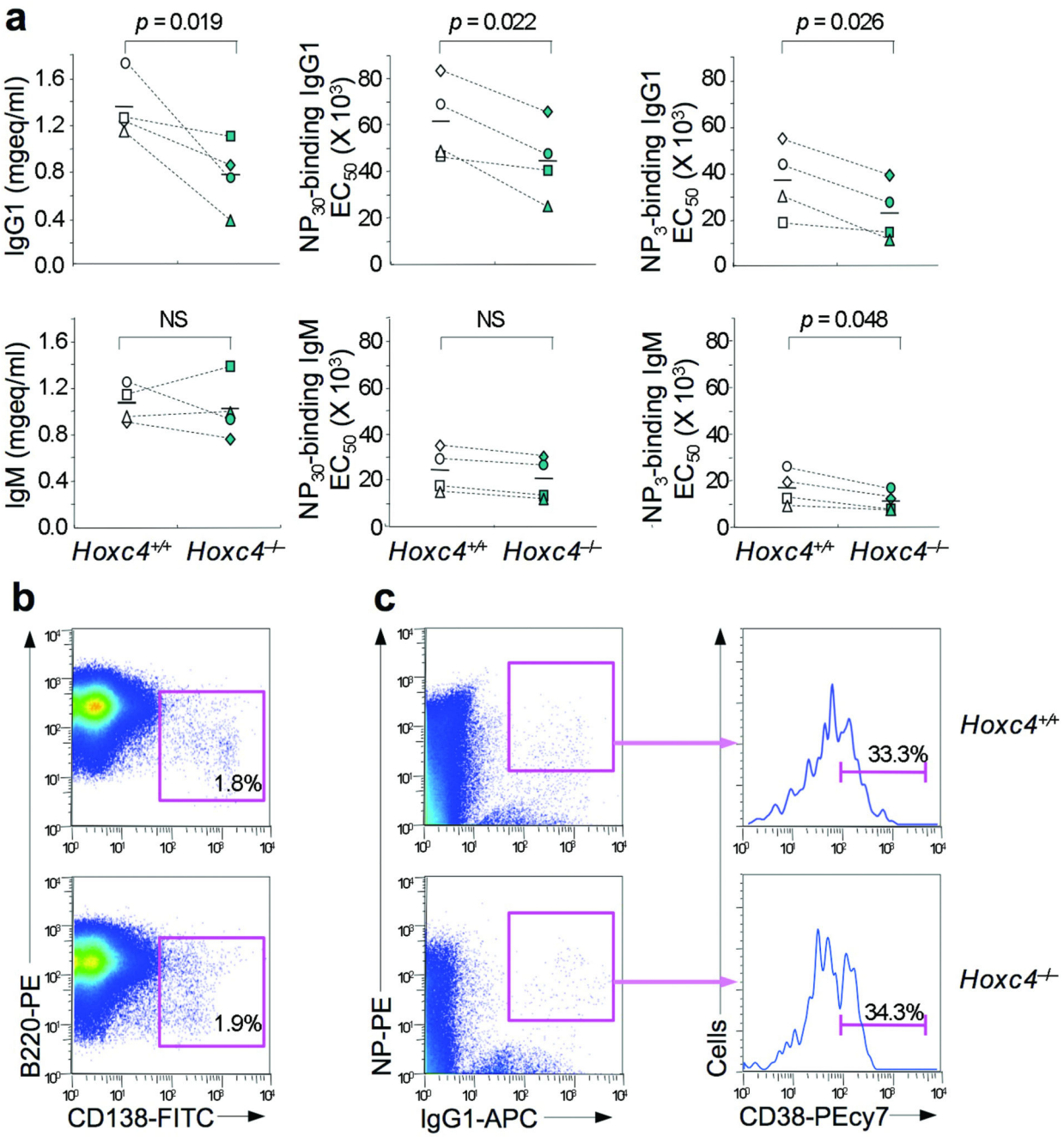

Figure 2.

Impaired antibody response in *Hoxc4*$^{-/-}$ mice. (**a**) Four pairs of littermate *Hoxc4*$^{+/+}$ and *Hoxc4*$^{-/-}$ mice were immunized with NP_{16}-CGG and boost-injected 21 d later. Circulating IgM and IgG1, NP_{30}-binding IgM and IgG1, and (high-affinity) NP_3-binding IgM and IgG1 were measured 7 d after the boost-injection, and, their levels were expressed as 50% effective concentration (EC_{50}) units. These were defined as the number of dilutions needed to reach 50% of saturation binding. (**b** and **c**) Normal plasma cell and memory B cell development in *Hoxc4*$^{-/-}$ mice 14 d after immunization with NP_{16}-CGG. (**b**) Surface

CD138 and B220 expression in spleen cells from immunized littermate *Hoxc4*$^{+/+}$ and *Hoxc4*$^{-/-}$ mice. Numbers in boxes are B220^{lo} CD138^{+} (plasma) cells, as percentage of total B220^{+} cells. (**c**) Spleen cells from immunized littermate *Hoxc4*$^{+/+}$ and *Hoxc4*$^{-/-}$ mice were analyzed by flow cytometry after staining with FITC-PNA, APC-anti-mouse IgG1 mAb, PE-NP and PECy7-anti-mouse CD38 mAb. Insets in left panels show NP-binding surface IgG1^{+} B cells. Right panels show CD38 expression by the gated NP-binding IgG1^{+} B cells. Data are representative of 3 independent experiments (**b** and **c**).

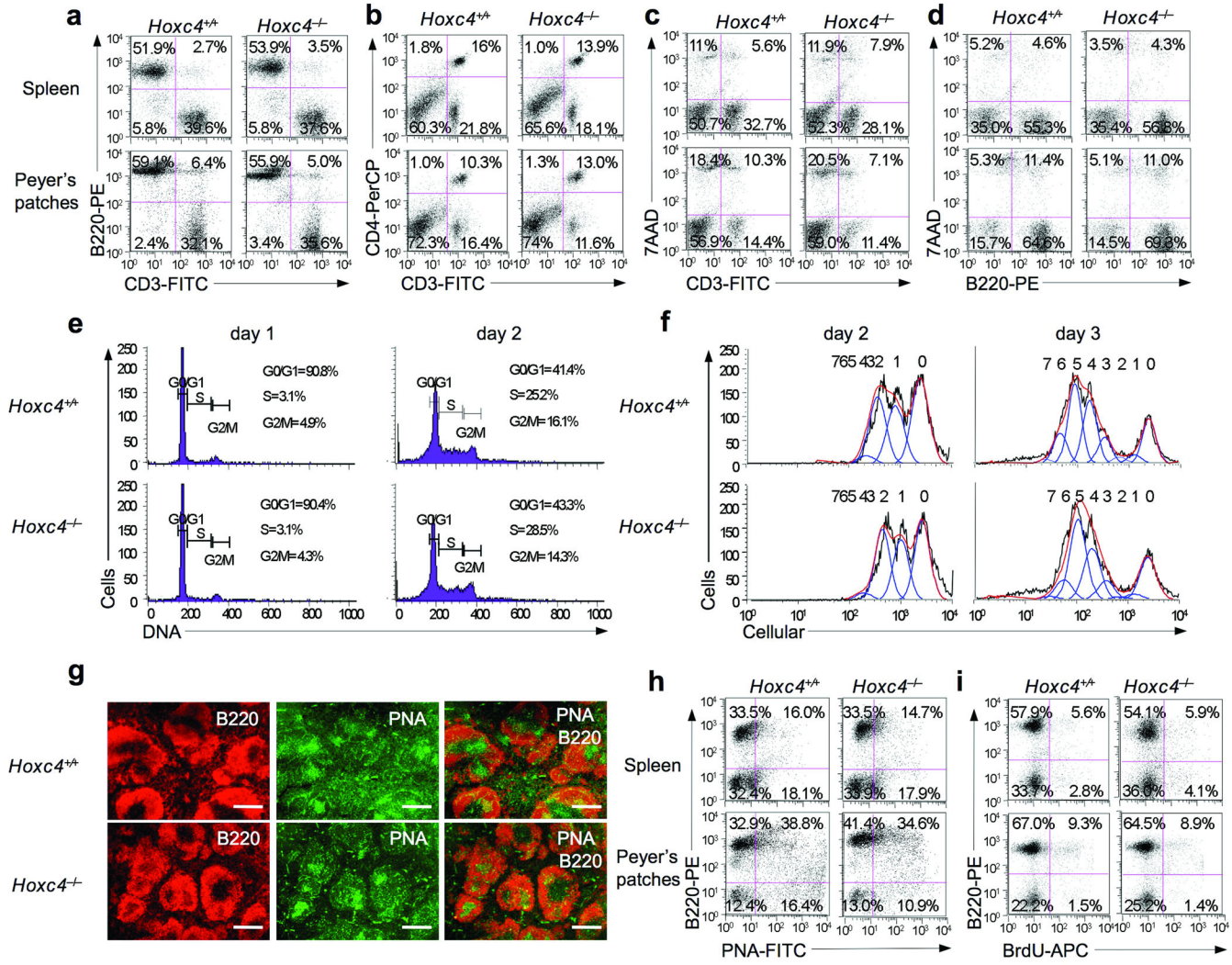

Figure 3.

HoxC4 deficiency does not affect B and T cell numbers, $CD4^+$ T cell numbers, B and T cell death in spleen and Peyer's patches, B cell cycle or division, nor does it alter GC formation and *in vivo* B cell proliferation. (**a–d**) Flow cytometric profiles of cells from spleen and Peyer's patches stained with (**a**) PE-anti-B220 mAb and FITC-anti-CD3 mAb, (**b**) FITC-anti-CD3 mAb and PerCP-anti-CD4 mAb, (**c**) 7-AAD and FITC-anti-CD3 mAb, and (**d**) 7-AAD and PE-anti-B220 mAb. (**e**) Cell cycle analysis of $Hoxc4^{+/+}$ and $Hoxc4^{-/-}$ B cells. Spleen $Hoxc4^{+/+}$ and $Hoxc4^{-/-}$ B cells were stimulated with LPS and IL-4 and harvested after 1 and 2 d for PI staining and flow cytometry analysis to measure DNA content and enumerate cells in G0/G1, S and G2/M phases. (**f**) Cell division in $Hoxc4^{+/+}$ and $Hoxc4^{-/-}$ B cells. Spleen $Hoxc4^{+/+}$ and $Hoxc4^{-/-}$ B cells were labeled with CFSE, cultured with LPS and IL-4, and harvested 2 and 3 d later for flow cytometry analysis. Cell division is indicated by progressive left shift of fluorescence histograms. Individual cell generations are enumerated above the graph. Data are from one representative of 3 experiments. (**g**) Staining of GCs in spleen sections prepared 10 d after immunization of $Hoxc4^{+/+}$ and $Hoxc4^{-/-}$ mice. Scale bar: 200 μm. The original magnifications are indicated at the bottom of each set of panels. (**h**)

Flow cytometric profiles of cells from Peyer's patches from NP_{16}-CGG immunized *Hoxc4*$^{+/+}$ and *Hoxc4*$^{-/-}$ mice stained with PE-labeled anti-B220 mAb and FITC-PNA. (**i**) *In vivo* B cell proliferation. Three 10-week-old *Hoxc4*$^{+/+}$ and *Hoxc4*$^{-/-}$ mice were immunized with NP_{16}-CGG. After 10 d, the mice were injected with BrdU (1 mg) twice within 16 h and sacrificed 4 h after the last injection. Cells from spleen and Peyer's patches were stained with PE-anti-mouse B220 mAb or this mAb together with FITC-PNA. Incorporated BrdU was detected with APC-anti-BrdU mAb and analyzed using by FACS. Data are from one representative of 3 pairs of *Hoxc4*$^{+/+}$ and *Hoxc4*$^{-/-}$ mice.

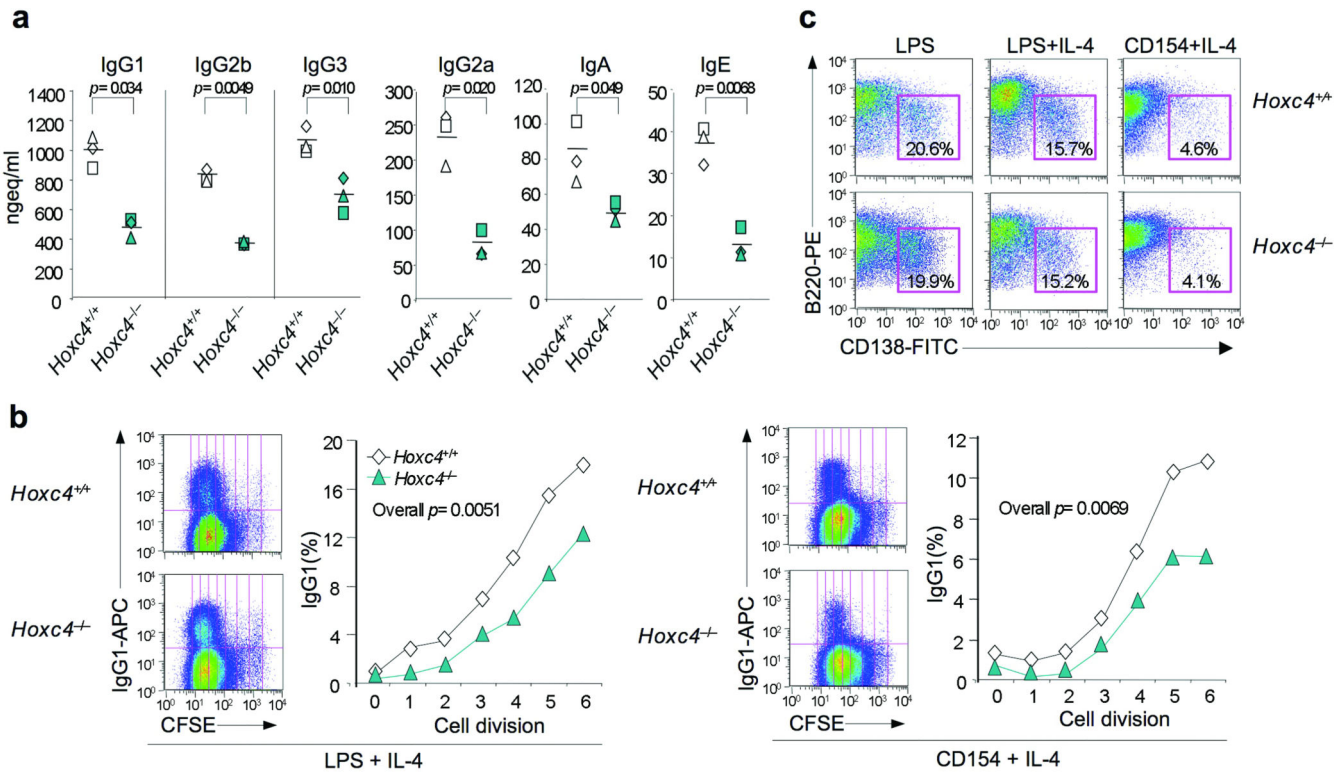

Figure 4.

Impaired CSR in *Hoxc4*$^{-/-}$ B cells. (**a**) Spleen *Hoxc4*$^{+/+}$ and *Hoxc4*$^{-/-}$ B cells were stimulated with LPS or CD154 in the presence of nil (for IgG2b and IgG3), IL-4 (for IgG1 and IgE), IFN-γ (for IgG2a), or TGF-β1/IL-4/IL-5/anti-δ mAb-dextran (for IgA). After 7 d, the supernatants from the cultures of *Hoxc4*$^{+/+}$ B cells (empty symbols) and *Hoxc4*$^{-/-}$ B cell (full symbols) stimulated with LPS or LPS and cytokines were collected and analyzed for concentration of different Ig isotypes. Data are from 4 pairs of *Hoxc4*$^{+/+}$ and *Hoxc4*$^{-/-}$ mice. (**b**) *Hoxc4*$^{+/+}$ and *Hoxc4*$^{-/-}$ B cells were labeled with cell division-tracking fluorochrome CFSE and stimulated with LPS and IL-4 or CD154 and IL-4 to induce switching to IgG1. This showed that proliferation of *Hoxc4*$^{-/-}$ B cells was normal. After 4 d of culture, *Hoxc4*$^{-/-}$ and *Hoxc4*$^{+/+}$ B cells completed the same number of divisions, but the percentage of surface IgG1^{+} B cells was significantly lower among *Hoxc4*$^{-/-}$ B cells. Data are from 2 independent experiments. (**c**) HoxC4 deficiency does not alter plasma cell differentiation. *Hoxc4*$^{+/+}$ and *Hoxc4*$^{-/-}$ B cells were stimulated with LPS, LPS and IL-4 or CD154 and IL-4. After 4 d of culture, the cells were stained with PE-anti-mouse B220 mAb and FITC-anti-mouse CD138 mAb for flow cytometry analysis. Numbers in boxes indicate B220^{lo}CD138^{+} (plasma) cells as percentage of total cells analyzed. Data are from one representative of 3 independent experiments.

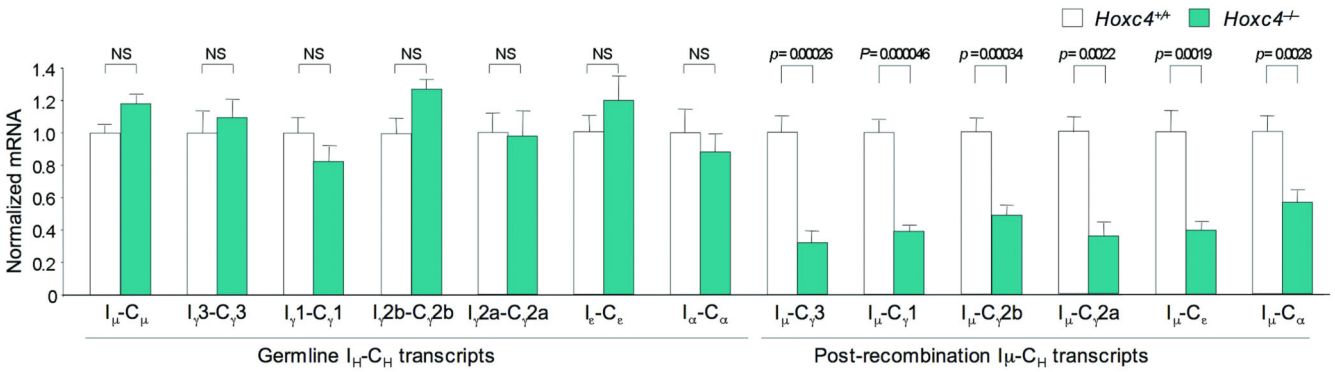

Figure 5.

HoxC4 deficiency does not alter germline I_H-C_H transcripts but reduces the expression of post-recombination Iμ-C_H transcripts. Spleen *Hoxc4*$^{+/+}$ and *Hoxc4*$^{-/-}$ B cells were cultured with LPS or LPS and cytokines for 3 d and then harvested for RNA extraction. This was used as template in real-time qRT-PCR to measure the levels of germline I_μ-C_μ, I_γ3-C_γ3, I_γ1-C_γ1, I_γ2b-C_γ2b, I_γ2a -C_γ2a, I_ε-$C_\varepsilon$and I_α-C_α transcripts, and post-recombination I_μ-C_γ3, I_μ-C_γ1, I_μ-C_γ2b, I_μ-C_γ2a, I_μ-C_ε and I_μ-C_α transcripts, as normalized to *CD79b* expression. Values are means ± s.e. (bars) of triplicate samples. Data are from one representative of 3 pairs of *Hoxc4*$^{+/+}$ and *Hoxc4*$^{-/-}$ mice. The data from the remaining 2 pairs are depicted in Supplementary Fig. 3.

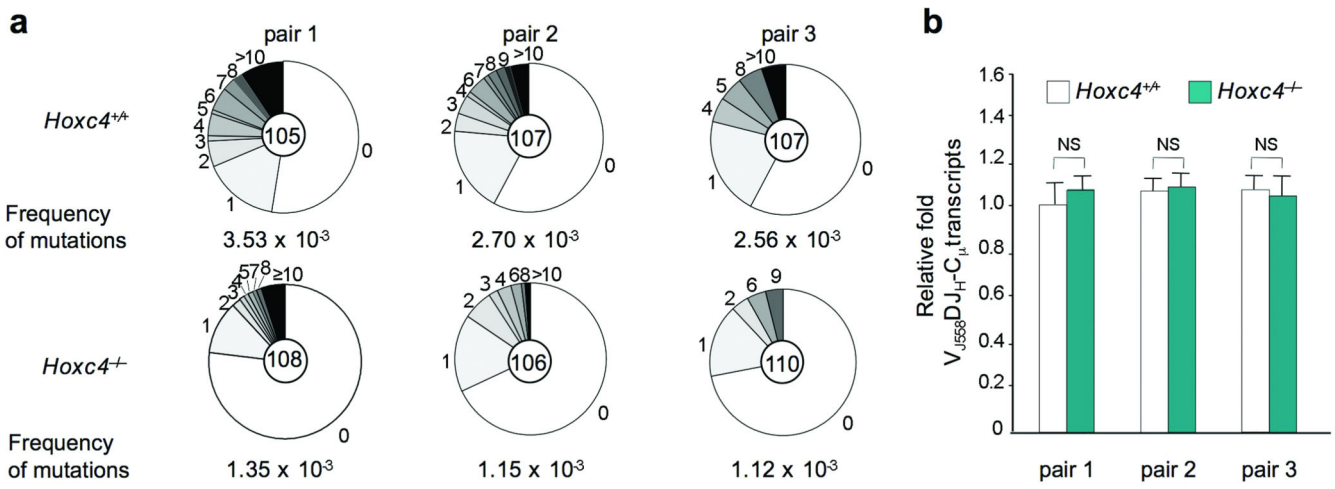

Figure 6.

Decreased somatic mutation frequency in the Ig H chain intronic J_H4-iEμ DNA of Peyer's patch $PNA^{hi}B220^+$ (GC) B cells from 3 12-week-old *Hoxc4*$^{-/-}$ mice as compare to their *Hoxc4*$^{+/+}$ littermates. (**a**) Pie charts depict the proportions of sequences that carry 1, 2, 3, etc. mutations over the 720 bp J_H4-iE_μ DNA analyzed. The numbers of the sequences analyzed are at the center of the pies. (**b**) HoxC4 deficiency does not alter the level of $V_{J558}DJ_H$-Cμ transcripts. $V_{J558}DJ_H$-C_μ transcripts in Peyer's patches B cells of these mice were measured by real-time qRT-PCR performed in triplicate samples using SYBR-green. In each sample, mRNA expression was normalized to *CD79b* expression. Data are means ± s.e. (bars) of triplicate samples from 3 independent pairs of *Hoxc4*$^{+/+}$ and *Hoxc4*$^{-/-}$ mice. The analysis of the spectrum of mutations in *Hoxc4*$^{+/+}$ and *Hoxc4*$^{-/-}$ mice is the subject of Supplementary Fig. 4.

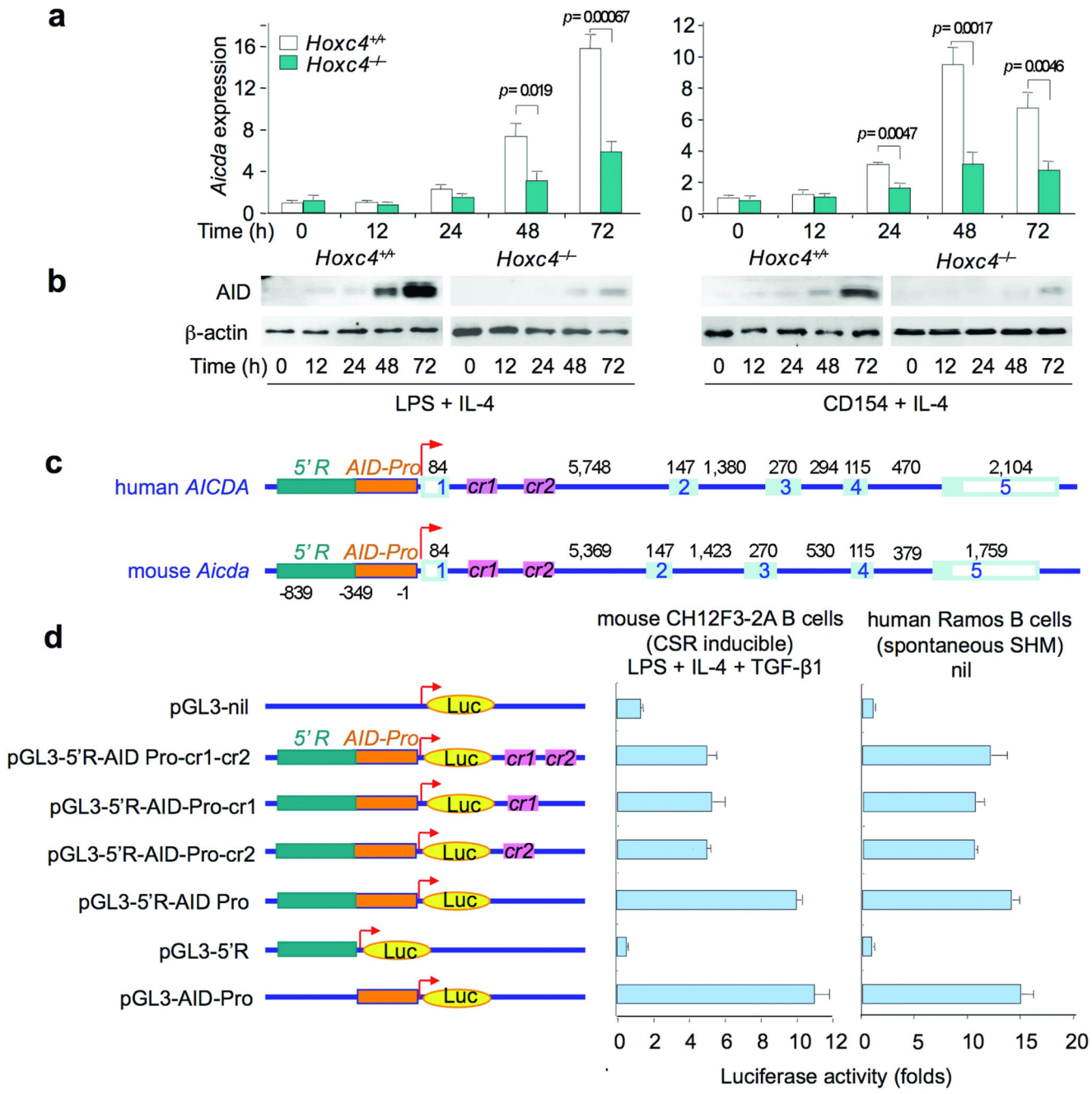

Figure 7.

(**a,b**) Decreased *Aicda* expression in *Hoxc4*$^{-/-}$ B cells. Spleen *Hoxc4*$^{+/+}$ and *Hoxc4*$^{-/-}$ B cells were cultured in the presence of nil, LPS and IL-4, or CD154 and IL-4. After 0, 12, 24, 48 and 72 h of culture, cells were harvested for RNA or protein extraction. (**a**) RNA (2 μg) was reverse-transcribed to cDNA and used as template in real-time qRT-PCR, in which *Aicda* expression was normalized to *CD79b* expression. Data are means ± s.e. (bars) of 3 independent experiments. (**b**) AID and β-actin proteins were detected by immunoblotting. Data are representative of 3 independent experiments. (**c**) Depicted, not to scale, are portion

of the human *AICDA* and mouse *Aicda* promoter region (*AID-Pro*), flanking 5' region (*5'R*), *cr1* and *cr2* in the first intron, and five exons, within which the coding region is depicted in light blue. (**d**) The −349 to −1 (*AID-Pro*) region, which we tentatively defined as *Aicda* promoter based on its high conservation, but not the immediately adjacent 5' region, nor the downstream *cr*1 or *cr*2 region promotes transcription. Human Ramos (undergoing spontaneous SHM) B cells and mouse CH12F3-2A (CSR inducible) B cells were transfected with the indicated pGL3-reporter gene vector to assess *Aicda* promoter activity. After transfection, CH12F3-2A cells were treated with LPS, IL-4 and TGF-β1 to induce CSR. Luciferase activity was measured after 16 h (Ramos) or 24 h (CH12F3-2A) of culture. Data are the means ± s.e. (bars) of 3 independent experiments.

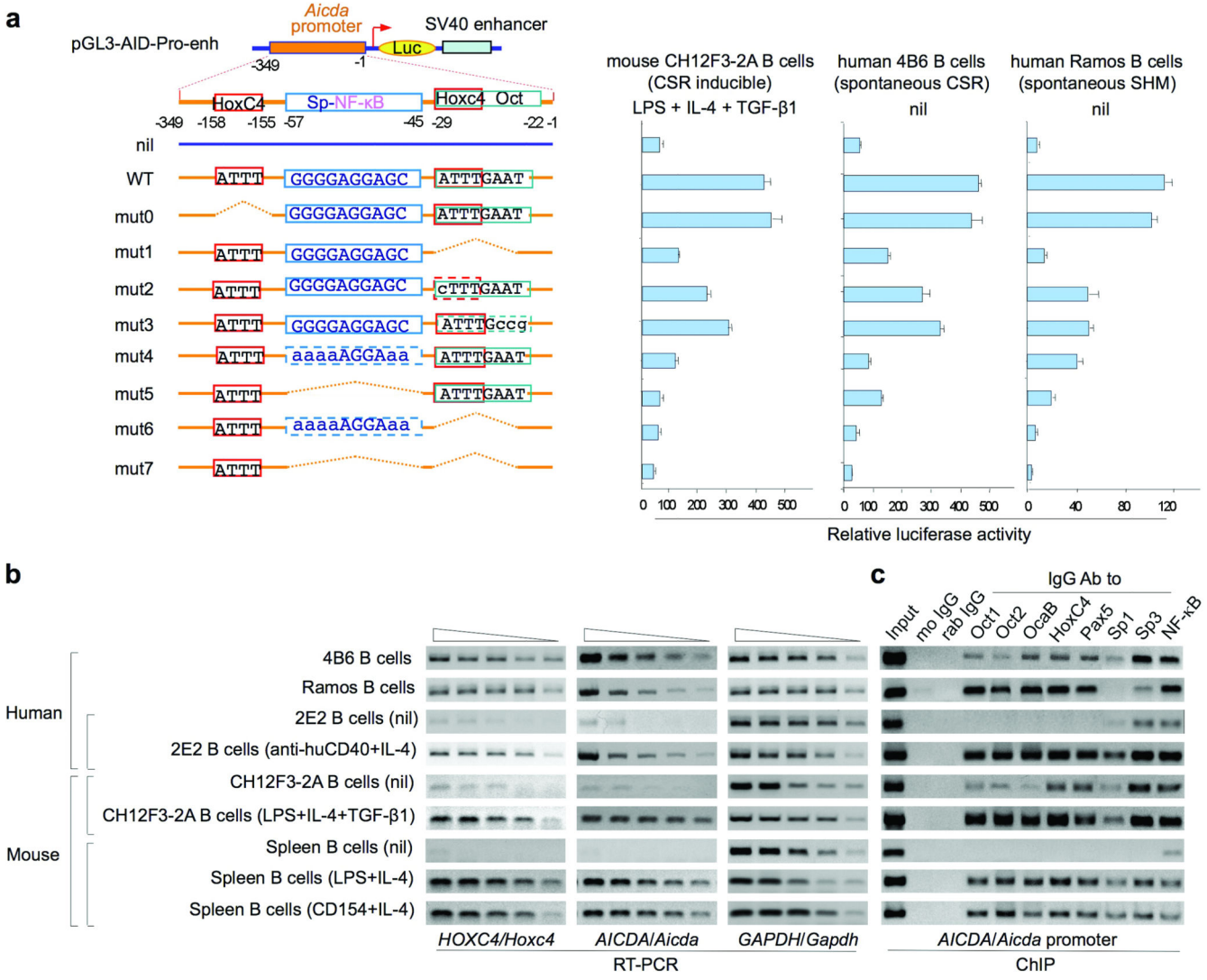

Figure 8.

The conserved HoxC4-Oct- and Sp-NF-κB-binding sites are essential for full *Aicda* promoter activity; HoxC4, Oct1, Oct2, OcaB, Pax5, Sp1, Sp3 and NF-κB (p52 subunit) are recruited to the *Aicda* promoter in B cells expressing *AICDA/Aicda* and undergoing CSR or SHM. (**a**) pGL3-Enhancer luciferase gene reporter constructs containing WT or mutant *Aicda* promoter, in which the HoxC4-Oct- and/or Sp-NF-κB-binding sites were deleted or disrupted by site-directed mutagenesis, were used to transfect CH12F3-2A, 4B6 or Ramos B cells. Luciferase activity was measured after 24 h (CH12F3-2A B cells) or 16 h (Ramos and 4B6 B cells) of culture. Data are means ± s.e. (bars) of 3 independent experiments. (**b**) *AICDA/Aicda* expression in human spontaneously switching 4B6 and Ramos B cells, human inducible switching 2E2 B cells stimulated with nil or anti-CD40 mAb and IL-4, mouse CH12F2-2A B cells stimulated with nil or LPS, IL-4 and TGF-β1, WT C57BL/6 mouse spleen B cells stimulated nil, LPS and IL-4, or CD154 and IL-4 were analyzed by semi-quantitative RT-PCR using serially two-fold diluted cDNA as a template. Data are representative of 3 independent experiments. (**c**) Cross-linked chromatin was precipitated

from the human or mouse B cells of panel **b** using a mouse mAb specific to HoxC4, rabbit Abs specific to Oct1, Oct2, OcaB, Pax5, Sp1, Sp3 or p52, or preimmune control mouse or rabbit IgG. The precipitated DNA was specified by PCR using *AICDA* or *Aicda* promoter primers. Data are representative of 3 independent experiments.

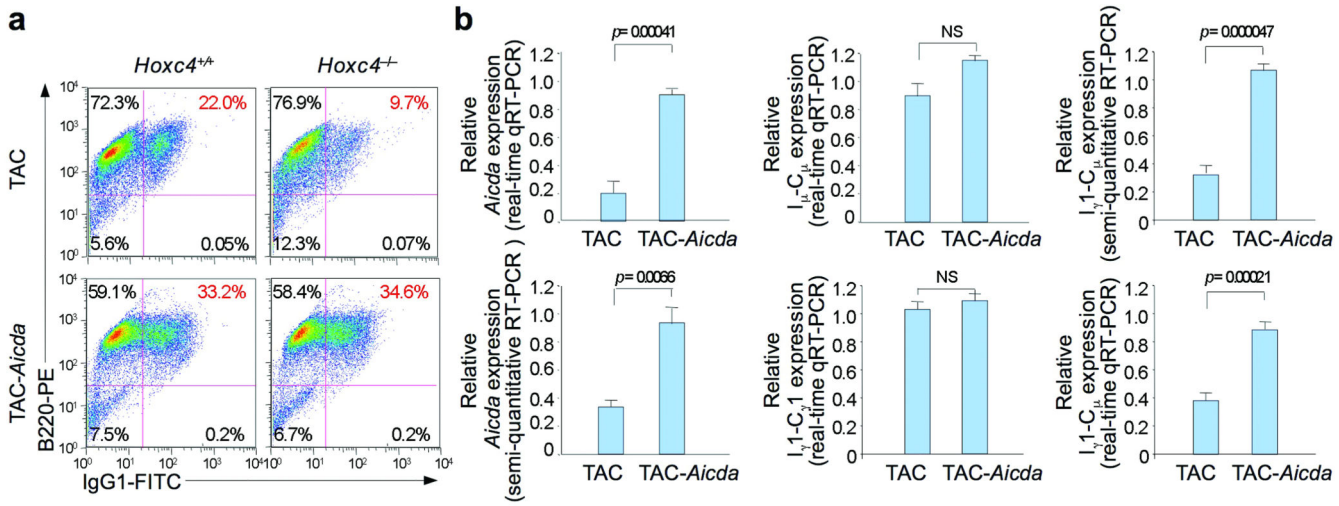

Figure 9.

Enforced expression of AID rescues CSR in *Hoxc4*$^{-/-}$ B cells. *Hoxc4*$^{+/+}$ and *Hoxc4*$^{-/-}$ B cells activated with LPS were transduced with the TAC control or AID-expression TAC-*Aicda* retrovirus and cultured in the presence of LPS and IL-4. Three or 4 d after transduction, B cells were harvested for analysis of surface expression of B220 and IgG1 (**a**) and expression of *Aicda* by real-time qRT-PCR and semi-quantitative RT-PCR, germline I_μ-C_μ and $I_\gamma 1$-$C_\gamma 1$ transcripts by real-time qRT-PCR, circle $I_\gamma 1$-C_μ transcripts by semi-quantitative RT-PCR and post-recombination I_μ-$C_\gamma 1$ transcripts by real-time qRT-PCR (**b**). Expression of these transcripts was normalized in each case to *CD79b* transcripts; expression of transcripts in *Hoxc4*$^{-/-}$ B cells were depicted as ratios to those in *Hoxc4*$^{+/+}$ B cells. FACS data are from one representative of 5 independent experiments. Real-time qRT-PCR and semi-quantitative RT-PCR data are means ± s.e. (bars) of 3 independent experiments.